the Energy to Lead

QUARTERLY REPORT

GTI PROJECT NUMBER 20916

Modeling of Microbial Induced Corrosion on Metallic Pipelines Resulting from Biomethane and the Integrity Impact of Biomethane on Non-Metallic Pipelines

DOT Prj# 293

Contract Number: DTPH56-09-T-000002

Reporting Period:
5th Project Quarter

Report Issued (Period Ending):
December 31, 2010

Prepared For:
U.S. Department of Transportation Pipeline and Hazardous Materials Safety Administration
Anthony Rallis
Technical Manager
Office of Pipeline Safety/Southwest Region
713-272-2835
Anthony.rallis@dot.gov

Prepared By:

GTI Project Team:
Joe Baffoe, Karen Crippen, Daniel Ersoy, Brian Spillar, Nick Daniels, Monica Ferrer, Zhongquan Zhou, Xiangyang Zhu

Kristine Wiley, *Team Project Manager*
Kristine.wiley@gastechnology.org
847-768-0910

Gas Technology Institute
1700 S. Mount Prospect Rd.
Des Plaines, Illinois 60018
www.gastechnology.org

Legal Notice

This information was prepared by Gas Technology Institute ("GTI") for DOT/PHMSA (Contract Number: DTPH56-09-T-000002.

Neither GTI, the members of GTI, the Sponsor(s), nor any person acting on behalf of any of them:

a. Makes any warranty or representation, express or implied with respect to the accuracy, completeness, or usefulness of the information contained in this report, or that the use of any information, apparatus, method, or process disclosed in this report may not infringe privately-owned rights. Inasmuch as this project is experimental in nature, the technical information, results, or conclusions cannot be predicted. Conclusions and analysis of results by GTI represent GTI's opinion based on inferences from measurements and empirical relationships, which inferences and assumptions are not infallible, and with respect to which competent specialists may differ.

b. Assumes any liability with respect to the use of, or for any and all damages resulting from the use of, any information, apparatus, method, or process disclosed in this report; any other use of, or reliance on, this report by any third party is at the third party's sole risk.

c. The results within this report relate only to the items tested.

Table of Contents

Page

Legal Notice ii
Table of Contents iii
Table of Tables iv
Table of Figures v
Project Objective 1
List Activities/Deliverables Completed During Reporting Period 2
Technical Status 2
Task 3 - Lab Evaluation of Microbial Corrosion under Simulated Field Conditions 2
Conditions for Modeling Experiments 2
Microbial consortium 3
Artificial growth medium 4
Preparation of Bacteria Consortium 5
Growth of Bacillus licheniformis under various conditions 5
Preparation of baseline bacteria culture from condensate sample 8
Final bacteria consortium and growth medium for corrosion experiments 8
Instrumentation for Modeling Data Collection 10
Electrodes and electrochemical cells 11
Electrochemistry and data acquisition 14
Test Protocol for Electrochemical Measurement of Microbial Corrosion 15
Sterilization and assembly of electrochemical cells 15
Test protocol 16
Task 8 - Perform Bounded Testing to Generate a Strong Example Data Set 21
Protocol for Biogas Collection 22
FuelMaker FM4 Compressor 22
Considerations for Gas Sampling at Biogas Plants 22
Biogas/Biomethane Gas Sample Sites 23
Gas Saturation Test Setup 23
Test Materials 23
NBR and SBR Rubber Sheet Materials 23
Natual Gas Sample 23
Biogas/Biomethane Samples 23
References 30

Table of Tables

Page

Table 1. Artificial Growth Medium Recipe for Corrosion Experiments..... 4

Table 2. The Closest Relatives of Heterotrophic Bacteria Sequences Isolated from Final Bacteria Consortium after Incubation of Various of Hours at 30 ºC, using Universal Primers Targeting 16S rRNA Gene 10

Table 3. Properties of AMG.....10

Table 4. The Properties of NBR and SBR Rubber Sheet Mateirals 24

Table 5. Chemical Compositions (approximate) of Gas Samples.....25

Table of Figures

Page

Figure 1. Growth curve of *B. licheniformis* in 0.8% nutrient broth under aerobic conditions. 6

Figure 2. Growth curve of *B. licheniformis* in 0.8% nutrient broth under 0.7% oxygen. 7

Figure 3. Growth curve of *B. licheniformis* in AGM supplemented with 0.3% nutrient broth under 0.7% oxygen. 8

Figure 4. Growth curve of enrichment culture of field condensate in AGM supplemented with 0.3% nutrient broth under 0.7% oxygen. 9

Figure 5. Top view of anodic cell. 12

Figure 6. Side view of anodic cell. W.E.: working electrode; C.E.: counter electrode; R.E.: reference electrode. 12

Figure 7. Top and side view of cathodic cell. 13

Figure 8. The assembled two-cell electrochemical system. 13

Figure 9. Setup and connections of electrochemical cells. 14

Figure 10. Anaerobic bacteria culturing system incorporated with InterCorr SmartCET electrochemical device for real-time corrosion monitoring 17

Figure 11. Actual B value determined by InterCorr SmartCET Instrument 18

Figure 12. Electrochemical test setup to monitor potential difference between anode and cathode. 20

Figure 13. Electrochemical test setup to verify potential difference between A1 and A2. 20

Figure 14. Electrochemical test cell setup for current and corrosion rate monitoring. 21

Figure 15. Biogas Collection Schematic (Updated) 26

Figure 16. Gas Saturation Test Setup 27

Figure 17. Test Sample Cage 28

Figure 18. Pressure Vessel for Gas Saturation Test 29

Project Objective

The objective of this project is to understand key elements related to promoting the successful delivery of biomethane into natural gas pipeline networks. This project focuses on two key areas of concern: [1] the effect of microbial induced corrosion on metallic pipes and [2] the impacts of biogas/biomethane on a non-metallic gathering network from sustained biogas feedstock exposure. This report summarizes the work that has been conducted through the fourth quarter of 2010. Results from Tasks 3, and 8 are discussed in detail within this report.

List Activities/Deliverables Completed During Reporting Period

		SCH Date	CMPL Date
Task #3	Lab Evaluation of Microbial Corrosion	03/31/2011	In Progress
Task #8:	Perfom Bounded Testing	6/30/2011	In Progress

- Completed HazOp analysis for biogas/biomethane sample collection process.
- Completed Baseline Hazard Analysis for gas saturation testing.
- Finalized pressure test vessel design and completed building one test vessel.
- Identified the commercial plastic pipe and elastomer materials for testing.
- Identified the sites for biogas/biomethane sample collection.

Technical Status

Task 3 - Lab Evaluation of Microbial Corrosion under Simulated Field Conditions

Conditions for Modeling Experiments

Corrosion is mainly the consequence of electrochemical reactions, influenced by the physico-chemical environment at the metal surface, such as oxygen, salts, pH, redox potential, and conductivity, etc. MIC is electrochemical corrosion influenced by the presence or activities of microorganisms. Microorganisms growing at the metal surface form a biofilm and release chemicals or electrochemically active minerals, which alter the rates and types of electrochemical reactions at the biofilm-metal interface and result in various types of corrosions (e.g. pitting, crevice corrosion, under-deposit corrosion, and galvanic corrosion)

Biogas, generated through the anaerobic digestion from a variety of biomass sources, is one of the fastest growing renewable fuels. Within the past few years, there has been enthusiasm and investment in bioconversion of waste products into quality fuel, encouraged by political and public pressure to create and use “green” energy products. Local gas distribution companies (LDCs) are poised to take delivery of (interchange) cleaned biomethane into their existing lines for general distribution. However, based upon its source (dairy waste, landfill, wastewater sludge, agricultural waste, etc.), biogas may contain constituents that may affect pipeline integrity and system operations, and possibly impede pipeline safety. One such known constituent is bacteria associated with microbiologically-induced corrosion (MIC) in the biogas carried over from the anaerobic digestion process. However, the relationship between the numbers of specific MIC bacteria introduced into the pipe, internal pipe conditions, and severity of metallic pipeline corrosion has not been fully understood [12, 132] despite the fact that MIC has been long recognized as one of the major causes of corrosion of metal pipes [7, 23, 30, 31].

Raw biogas, saturated with moisture, contains hundreds of live bacteria including those known to cause MIC (e.g., APB, IOB, and SRB) from the anaerobic digestion process. The

properties of condensate formed in gathering pipeline are affected by biogas composition (CO_2 and H_2S, etc), dissolved chemicals and nutrients from the anaerobic digestion process, which in turn, influence the dominant bacterial profile and microbial interactions with the metal surfaces. The potential impact of microbial corrosion on the integrity of metallic gathering pipelines must be addressed.

Consequences of the direct introduction of live microbes to metallic pipeline networks are unknown. A clear understanding of such potential integrity impact is crucial to safe introduction of biogas into metallic natural gas networks. In addition, a predictive tool to foretell MIC severity under field conditions is necessary for the effective management of pipeline integrity, especially for gathering lines containing the raw biogas.

Internal corrosion in raw biogas lines are affected by many factors or combination of factors including CO_2, H_2S, organic acid (mainly acetic acid), microbes, oxygen, chloride, etc. The focus on a single mechanism such as microbial corrosion is therefore not appropriate or practical in an actual pipeline system [133]. The development of the MIC model has to include other factors which may interact with microbial activities and their metabolites, and change electrochemical characteristics at the metal-biofilm interface. Parameters which affect microbial growth and activities will probably affect the onset of microbial corrosion (i.e. pitting), corrosion rate and severity. The parameters which may be included in the MIC model are nutrients (sulfate, fatty acids, total dissolved solids, utilizable nitrogen), CO_2, H_2S, O_2, pH of condensate, salinity, alkalinity, dissolved iron, sulfide, chlorides, bicarbonates, ferrous and ferric iron, and temperature. The final parameters which were included in our preliminary MIC model were determined based on the results from Task 1 literature review and Task 2 sample analyses.

The major bacterial populations in raw biogas and condensate samples collected from gathering lines have been determined in Task 2, and the results used to formulate a major corrosion-related bacteria consortium to evaluate the microbial corrosion of metallic pipelines. In addition, chemical compositions and properties of typical condensate in raw biogas gathering line were thoroughly analyzed in Task 2. Therefore, the microbial corrosion evaluation was performed in synthetic condensate to mimic the field conditions typically found in raw biogas gathering line.

Microbial consortium

The accurate diagnosis of MIC requires combination of microbiological, chemical, and metallurgical analyses. The microbiological indicators include detection and quantification of various microorganisms on metal-liquid interfaces, especially corrosive bacteria in biofilms formed on metal surfaces.

qPCR assays indicated that most of raw biogas samples contained two types of corrosion-causing bacteria – APB and IOB, and the condensate sample mainly contained APB. However, after the raw biogas samples were inoculated in TG media and incubated for 7 days at 37 ºC, qPCR on positive growth cultures indicated the presence of overwhelming number of APB in most of samples (data not shown). The identities of most sequences of heterotrophic bacteria or bacterial spores in raw biogas were closely related to the sequences of two bacteria genera, i.e. *Paenibacillus* and *Bacillus*. Species determination of corrosion-related bacteria showed the

presence of *Clostridium* and *Acidovorax* species, in addition to dominant *Paenibacillus* and *Bacillus* species. IOB such as *Gallionella*, *Leptothrix*, and *Sphaerotilus* might not be a significant corrosion-related population in raw biogas samples. From the condensate sample, the dominant heterotrophic bacteria species were also closely related to *Bacillus* and *Paenibacillus*, though after growth in TG medium, the dominant bacteria species changed to *H. saxobsidens*.

The majority of sequences isolated from this project are closely related to the sequences of genus *Bacillus*, followed by *Paenibacillus*, and *Clostridium*. Of all the sequences from these three genera, *Bacillus* sequences accounted for approximately 71.4%, *Paenibacillus* 24.3% and *Clostridium* 4.3%. The most representative *Bacillus* species is *B. licheniformis*. Therefore the proposed bacteria consortium which will be used in the corrosion experiment includes the enriched condensate culture (dominated by *H. saxobsidens*) and spiked *B. licheniformis.*

Artificial growth medium

The artificial growth medium (AGM) for corrosion experiments is based on the results of a thorough chemical analysis of the condensate sample and other nutrient requirements for bacteria growth such as trace elements and vitamins. In addition, nutrient broth will be added to the artificial medium during the corrosion experiment in attempt to support bacteria consortium growth at the rate that each electrochemical corrosion experiment can be completed in a reasonable time. The quantity of nutrient broth added to the medium will be determined through experiments on growth curves under various conditions. The AGM recipe (minus nutrient broth) is as following (Table 1).

Table 1. Artificial Growth Medium Recipe for Corrosion Experiments

Macronutrients	Milligram per L
NH_4HCO_3	400 mg
$Na_2HPO_4 \cdot H_2O$	30 mg
K_2SO_4	20 mg
$CaCl_2$	9 mg
$FeCl_2 \cdot 4H_2O$	5 mg
$MgSO_4 \cdot 7\ H_2O$	3 mg
100X Trace Elements stock (add 10 ml to 1 L)	Milligram per 100 mL
$MnCl_2 \cdot 4H_2O$	180
$CoCl_2 \cdot 6H_2O$	270
H_3BO_3	50
$CuCl_2 \cdot 2H_2O$	24
$NaMoO_4 \cdot 2H_2O$	23
$ZnCl_2$	19
100X Vitamins stock (add 10 ml to 1 L) *from ATCC Vitamin Supplement Formulation Catalog No: MD-VS	Milligram per 100 mL
Biotin	0.2
Folic Acid	0.2
Pyridoxine Hydrochloride	1.0
Riboflavin	0.5

Thiamin	0.5
Nicotinic Acid	0.5
B_{12}	0.01
p-Aminobenzoic Acid	0.5
Thioctic Acid	0.5
Calcium pantothenate	0.5
Monopotassium phosphate	0.5

Filter-sterilize macronutrients, 100X trace elements stock, and 100X vitamins stock individually. Store at 4 ºC until use.

Preparation of Bacteria Consortium

Based on thorough analysis of biogas and condensate samples, the bacteria consortium for MIC modeling experiment consists of *B. licheniformis* (ATCC 14580) and the baseline bacteria populations enriched from the field condensate sample. The thorough analysis of enrichment culture of condensate sample indicated the dominant presence of *H. saxobsidens*.

Bacillus licheniformis (ATCC 14580) are Gram-positive, rod-shaped, motile, aerobic endospore-forming thermophilic bacteria that hydrolyze sugars fermentatively. Colonies of *B. licheniformis* are round, surface smooth, flat, margin irregular and 2-4 mm in diameter. Ellipsoidal spores are produced in not swollen sporangia and placed centrally [129]. *B. licheniformis* is a common contaminant of dairy products; it is the most common aerobic spore-forming bacteria isolated from dairy farm [131]. The optimal growth temperature is around 50°C, though it can survive at much higher temperatures. *B. licheniformis* was purchased from American Type Culture Collection (ATCC14580) for this project.

Herminiimonas saxobsidens are Gram-negative, rod-shaped bacteria. Cells are motile by means of polar flagella, non-sporulating and strictly aerobic. It utilizes acetate, propionate, oxalate, succinate and malate ions. The enriched condensate culture will be used to provide baseline bacteria population in corrosion experiments.

Growth of Bacillus licheniformis under various conditions

The growth curve of B. licheniformis was first performed in Nutrient Broth (BD Cat# 234000). A 5% volume of overnight culture inoculums was inoculated into NB medium and the culture tubes were incubated aerobically or under 0.7% of O2 in headspace at 30 C with 100 rpm shaking. Absorbance/OD was measured at 600 nm periodically and the OD reading was plotted against time of incubation to generate a growth curve for the bacteria. The growth curves under various conditions are shown in Figure 1 through Figure 3. *B. licheniformis* growth curve in NB medium under aerobic condition showed an exponential growth phase between 5 and 13 hrs after incubation at 30 C (Figure 1).

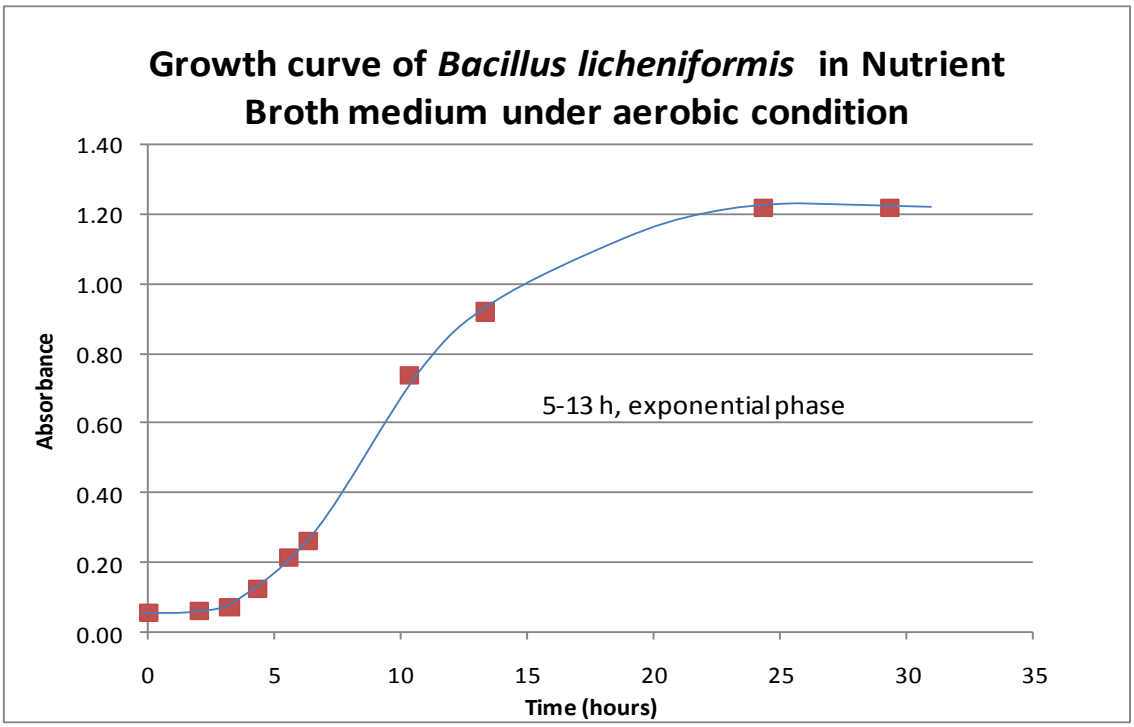

Figure 1. Growth curve of *B. licheniformis* in 0.8% nutrient broth under aerobic conditions.

Typical raw biogas line is not strictly aerobic or anaerobic; it contains an average of 0.7 Mol% of oxygen based on 12 raw biogas samples collected. The presence of oxygen in the raw biogas line explains why the dominant bacteria isolated from the samples are aerobic bacteria or facultative anaerobic bacteria, such as *B. licheniformis*, *P. barengoltzii*, *H. saxobsidens* (aerobes), and *P. glucanolyticus* (facultative anaerobe). In order to mimic raw biogas line condition, the growth curve of *B. licheniformis* was repeated under conditions in presence of 0.7% of O_2 in headspace of culture bottles. The medium was purged with gas containing 94.3% N_2-5% H_2-0.7% O_2 to create the growth conditions for the bacteria. The growth curve under 0.7% of oxygen is shown in Figure 2. When aerobic *B. licheniformis* culture was incubated under 0.7% oxygen condition, *B. licheniformis* exhibited a longer lag growth phase (~12 hours), and reached lower OD readings (~0.3) within 24 hours of incubation at 30 ºC in 0.8% NB. The exponential growth phase was between 15 and 23 hours of incubation, about 10 hours later compared to aerobic conditions.

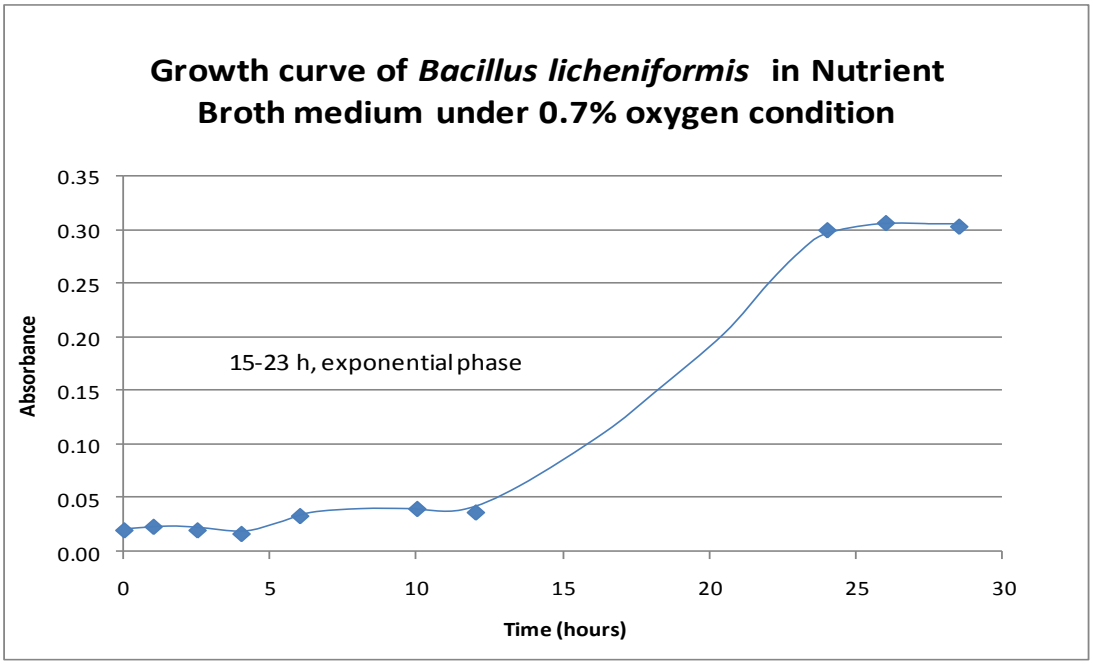

Figure 2. Growth curve of *B. licheniformis* in 0.8% nutrient broth under 0.7% oxygen.

When artificial growth medium (AGM) is used, it is necessary that AGM is supplemented with an appropriate percentage of NB in order to support bacterial consortium growth in corrosion experiments. The quantity of NB supplement required for growth of *B. licheniformis* was determined under 0.7% of headspace oxygen conditions at 30 ºC. The culture OD was monitored periodically to determine the growth potential at various concentrations of NB supplement. Under aerobic conditions, at least 0.3% of NB supplement to AGM was required to support the growth of *B. licheniformis*, with the highest OD (0.45) reached after 45 hours of incubation. However, under 0.7% O_2 condition, the highest OD was only 0.31 after 72 hours of incubation in AGM supplemented with 0.3% NB; the culture pH decreased from 7.6 at the beginning to 7.24 after 168 hours. A more detailed growth curve was determined for *B. licheniformis* in AGM supplemented with 0.3% of NB and under 0.7% O2 at 30 ºC in Figure 3. *B. licheniformis* showed an exponential growth phase during 15-40 hours of incubation, with the highest OD (0.32) reached after 156 hours of incubation.

Therefore, *B. licheniformis* culture prepared in AGM supplemented with 0.3% of NB under 0.7% of headspace oxygen will be used to prepare bacteria consortium for corrosion experiments.

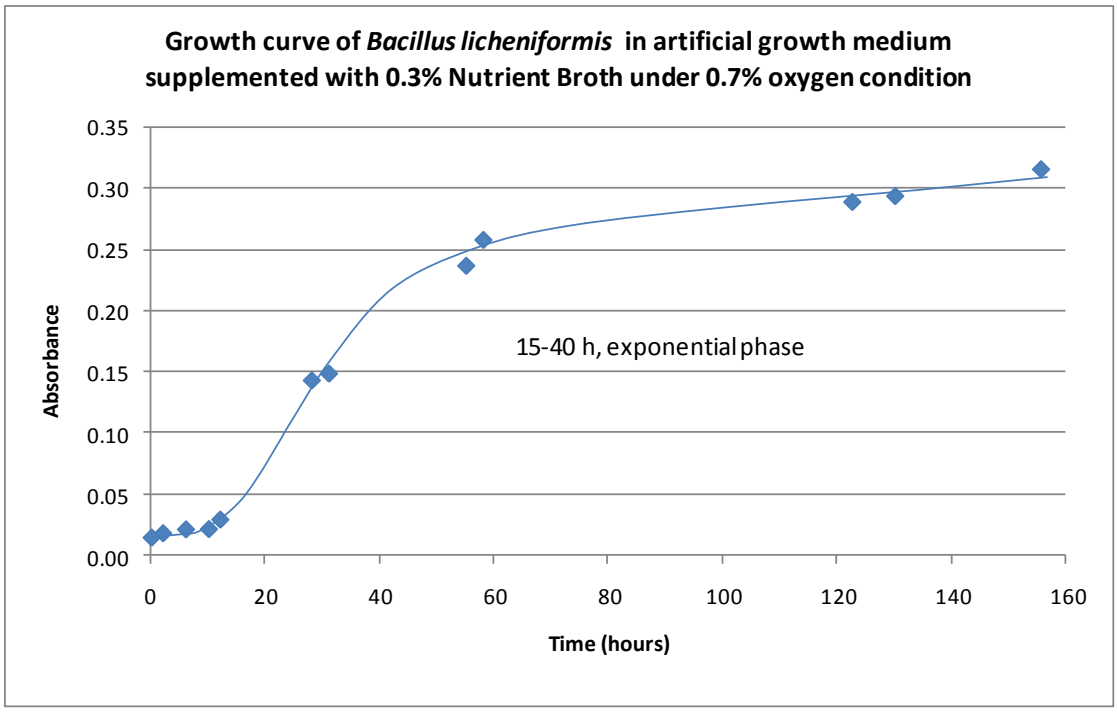

Figure 3. Growth curve of *B. licheniformis* in AGM supplemented with 0.3% nutrient broth under 0.7% oxygen.

Preparation of baseline bacteria culture from condensate sample

A 5% volume of field condensate sample was inoculated into AGM supplemented with 0.3% of NB and incubated under 0.7% of headspace oxygen at 30 ºC at 100 rpm shaking. Absorbance/OD was measured at 600 nm periodically and the OD reading was plotted with time of incubation to determine the exponential growth phase of the baseline bacteria population from the condensate sample. The field condensate sample showed an exponential growth phase between 15 and 30 hrs of incubation (Figure 4). The highest OD (0.14) was reached at 36 hours of incubation; then OD dropped to 0.12 after 156 hours of incubation.

Final bacteria consortium and growth medium for corrosion experiments

B. licheniformis and field condensate sample were grown in a large volume of AGM supplemented with 0.3% NB under 0.7% of headspace oxygen at 30 ºC at 100 rpm shaking. The cultures during exponential growth phase were collected and bacteria concentrations determined using the plate count method. The concentrations of *B. licheniformis* and field enrichment culture at exponential growth phase were 6.0 x 10^6/ml and 7.1 x 10^7/ml, respectively. The culture was then aliquoted and stored at 4 ºC until use.

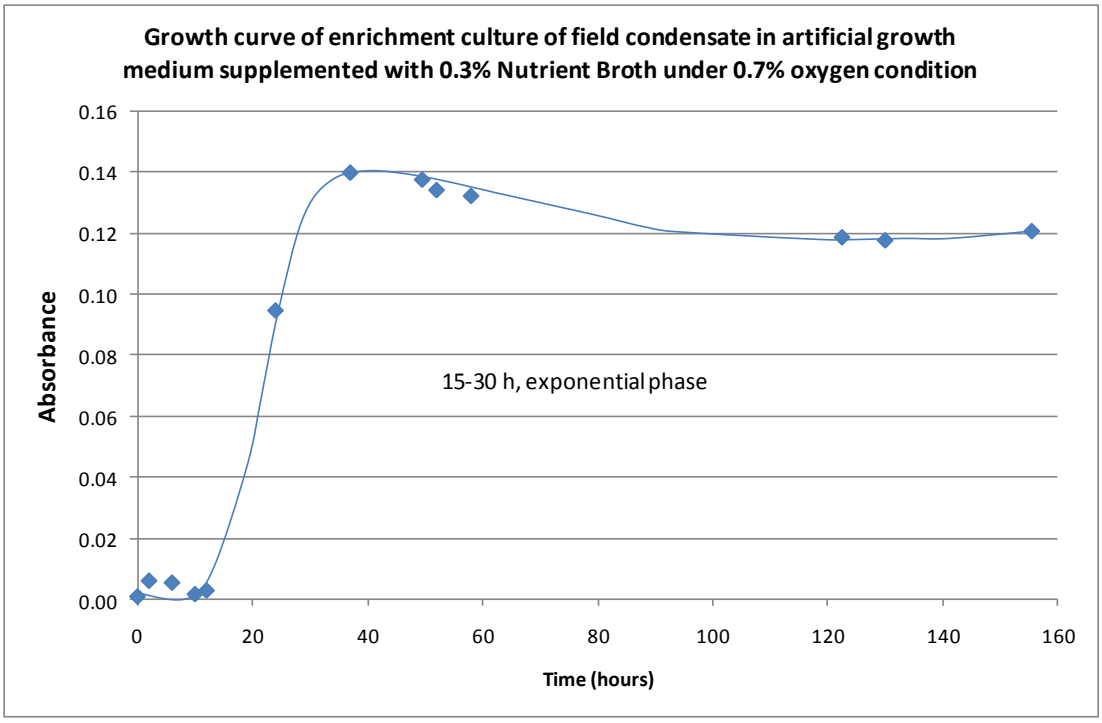

Figure 4. Growth curve of enrichment culture of field condensate in AGM supplemented with 0.3% nutrient broth under 0.7% oxygen.

The B. licheniformis and field enrichment culture were diluted to 1.0 x 10^6/ml and 1.0 x 10^7/ml, respectively, and then mixed at 1:1 ratio to create a final bacteria consortium, which contains 0.5 x 10^6/ml of *B. licheniformis* and 0.5 x 10^7/ml of baseline bacteria. 5% volume of the final consortium culture was inoculated into AGM supplemented with 0.3% NB under 0.7% of headspace oxygen at 30 ºC at 100 rpm shaking. The samples were taken after incubation of 0, 48, 96, and 168 hours, and the bacteria species determined using molecular method (PCR/Cloning/Sequencing). The change in the dominant bacteria communities in the final consortium after incubation is summarized in Table 2. At time 0, all 14 sequences were closely related to the dominant baseline bacteria *H. saxobsidens*. The composition of the bacteria consortium became more diverse after incubation at 30 ºC – acid-producing bacteria started to dominate the bacteria consortium and *H. saxobsidens* became the less dominant bacteria species over time.

The recipe of the AGM is the same as shown in Table 1. The AGM was supplemented with 0.3% of NB to support the bacteria consortium during electrochemical corrosion experiments. The pH and resistance are summarized in Table 3. A hydrophilic PVDF filter was used in the salt bridge to prevent the bacteria consortium in the anodic cell from entering the cathodic cell.

Table 2. The Closest Relatives of Heterotrophic Bacteria Sequences Isolated from Final Bacteria Consortium after Incubation of Various of Hours at 30 ºC, using Universal Primers Targeting 16S rRNA Gene

Hours after incubation	Closest relative in Genbank	Genbank accession No.	% Identity	Frequency
0	Herminiimonas saxobsidens	AB512141	99-100	3
	Herminiimonas saxobsidens strain NS11T	AM493906	99-100	11
48	Acidovorax sp. 'smarlab 133815'	AY093698	100	1
	Herminiimonas saxobsidens	AB512141	97-99	4
	Herminiimonas saxobsidens strain NS11T	AM493906	99-100	6
	Uncultured bacterium clone 1013-1-CG11	AY532539	98	1
	Uncultured bacterium clone EV818SWSAP79	DQ337095	98	1
	Uncultured bacterium, clone CAL_T6	FR675947	98	1
96	Acidovorax sp. 'smarlab 133815'	AY093698	99-100	4
	Bacillus licheniformis ATCC 14580	CP000002	99	1
	Bacillus licheniformis strain B8	EU117278	99	1
	Bacillus licheniformis strain CSB03	FJ189781	99	4
	Herminiimonas saxobsidens	AB512141	97-100	2
	Uncultured bacterium clone EV818SWSAP79	DQ337095	98	1
	Uncultured bacterium, clone: TS17	AB378588	98	2
168	Acidovorax sp. 'smarlab 133815'	AY093698	99	8
	Herminiimonas saxobsidens	AB512141	98-99	2
	Herminiimonas saxobsidens strain NS11T	AM493906	99	2
	Janthinobacterium sp. Marseille	CP000269	99	1
	Uncultured bacterium clone Hot Creek 44	AY168727	94	1
	Uncultured bacterium clone nbt05c05	EU535848	98	1

Table 3. Properties of AMG

	Resistance (KOhms)	pH
1X AGM	2.741	7.25
1X AGM with PVDF filter (0.1 µm)	2.958	
1X AGM + 0.3% NB	2.386	7.05
1X AGM + 0.3% NB with PVDF filter (0.1 µm)	2.563	

Instrumentation for Modeling Data Collection

Microbes are known to induce localized corrosion in deaerated conditions. Generally speaking, localized corrosion can be defined as the stabilization of a galvanic cell between a small anode that corrodes and a large cathodic surrounding area that is more or less protected. For microbiologically induced localized corrosion to occur, microbes such as SRB and APB not only have to initiate localized corrosion but also to stabilize it by sustaining a steady coupling current between small anodes and large cathodes [134]. Differential acidification is known to be one of the most powerful driving forces for localized corrosion [135]. Metabolites from microbial metabolism and the subsequent interaction between metabolites and corrosion products (e.g., the precipitation of iron sulfides) induce a differential acidification between anodes and

cathodes [136]. In addition, in the presence of CO_2 and H_2S, other effects can contribute to further local acidification and, especially, to the possible presence of conductive corrosion products [137, 138].

MIC has been studied mainly by electrochemical techniques that provide surface-averaged measurements. Techniques such as electrochemical impedance spectroscopy (EIS) or linear polarization give results, such as the uniform corrosion rate, that are not applicable to localized corrosion, including MIC [59]. Even electrochemical noise is not directly relevant to localized corrosion [139]. This noise is defined as the random process of pit nucleation between electrodes of reduced size. However, a pit nucleus is not yet an actual pit. Depending upon repassivation statistics, this initial step of pit nucleation may lead either to stable growth of a few pits or just a grainy surface in overall uniform corrosion [134]. On large electrodes, neither pit growth nor uniform corrosion is noisy because both are related to stable direct currents. The technique applied in this Task uses a multielectrode analyzer, a potentiostat/galvanostat, and a micro pH probe to measure potential, galvanic current, corrosion rate, and pH at the biofilm/metal interface under the influence of activities of a consortium of microorganisms. The data will be used to develop a preliminary model for prediction of microbiologically-induced corrosion under simulated conditions in raw biogas pipeline.

Electrodes and electrochemical cells

The electrodes are constructed of type C1018 carbon steel wire purchased from California Fine Wire Company. The diameter of the wire is 2 mm, and the chemical composition is (in weight%): Carbon 0.175%, Manganese 0.75%, Phosphorus 0.04%, Sulfur 0.05% with the balance Iron. The anode surface exposed to the liquid medium and bacteria is 3.14 mm^2. The cathode is made of coiled wire with exposed surface area of approximately 470 mm^2, resulting in a cathode to anode ratio of 150 to 1. The anode and cathode are insulated from the solution by heat shrink Teflon tubing and epoxy. Before starting an experiment, the electrodes are wet polished using silicon carbide (SiC) paper in sequence from 240-grit to 600-grit.

The electrochemical cell is a polycarbonate reaction vessel (2.5 L) with polycarbonate end plates to seal the vessel. The end plate has assorted ports for various electrochemical electrodes, pH probes, temperature probe, gas inlet and outlet for medium purging and headspace gas replacement, medium inlet and outlet for medium circulation, and inoculation ports [59]. Figure 5 and Figure 6 are top and side view of the anodic cell. The top and side view of the cathodic cell is shown in Figure 7. The anode electrodes are kept horizontal and facing up in the vessel since gravity has significant effect on bacterial attachment, and the horizontal surfaces facilitate bacterial adhesion [140, 141]. Membrane filters (0.2 µm) are placed at the gas inlet and outlet to protect the cell from external contamination. Figure 8 shows an assembled two-cell electrochemical system.

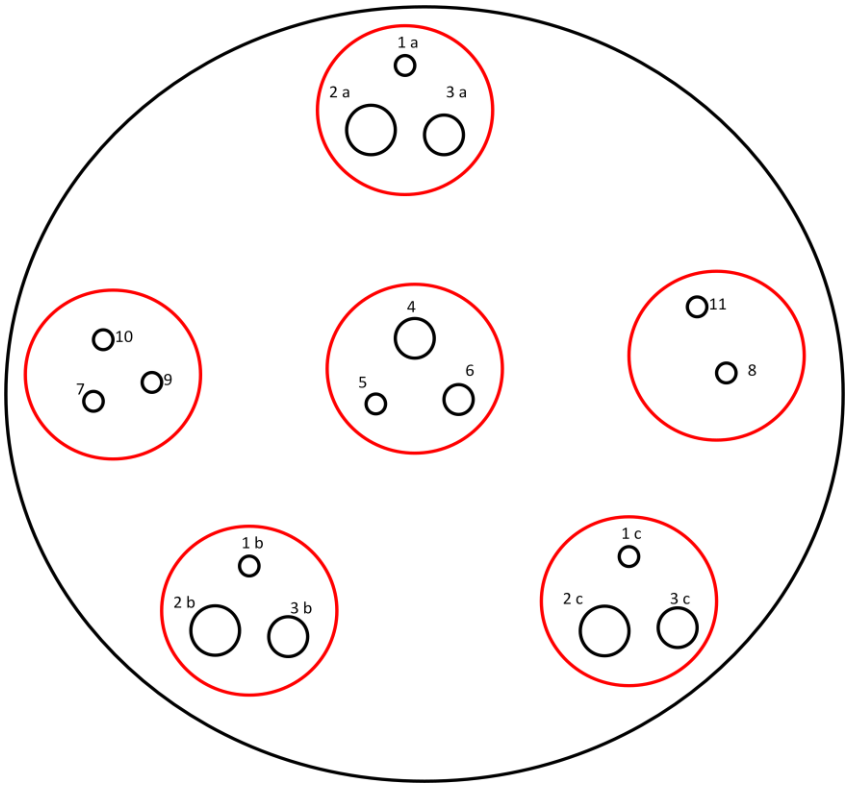

Figure 5. Top view of anodic cell.

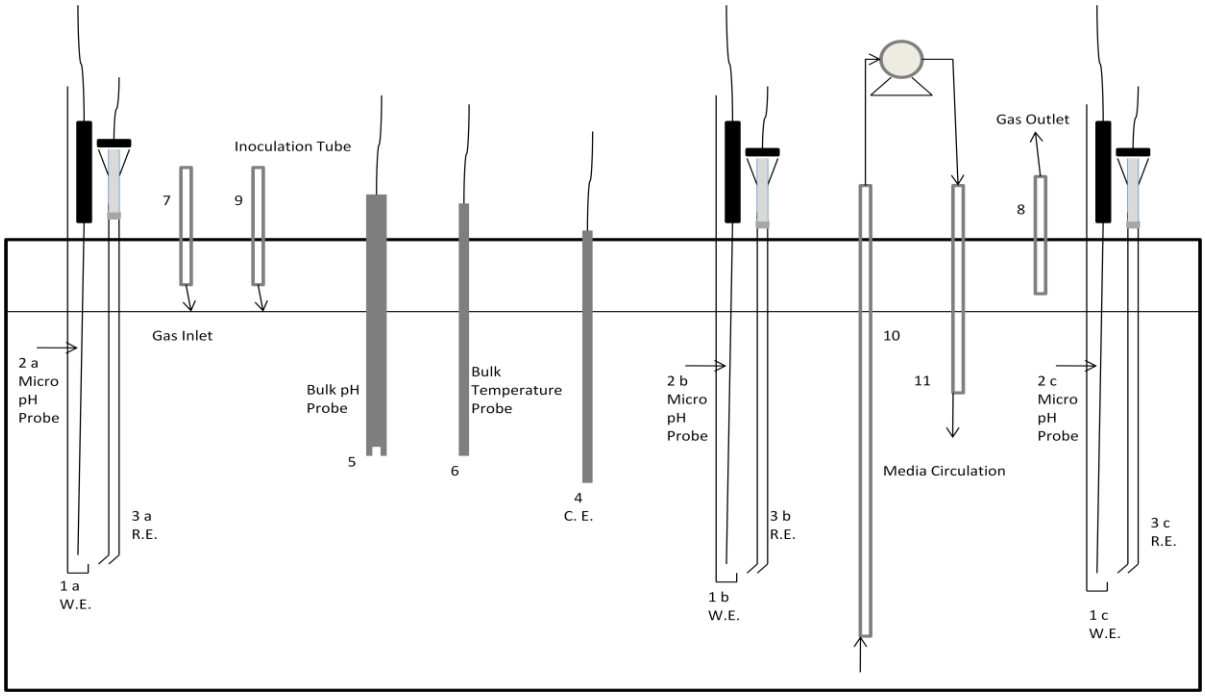

Figure 6. Side view of anodic cell. W.E.: working electrode; C.E.: counter electrode; R.E.: reference electrode.

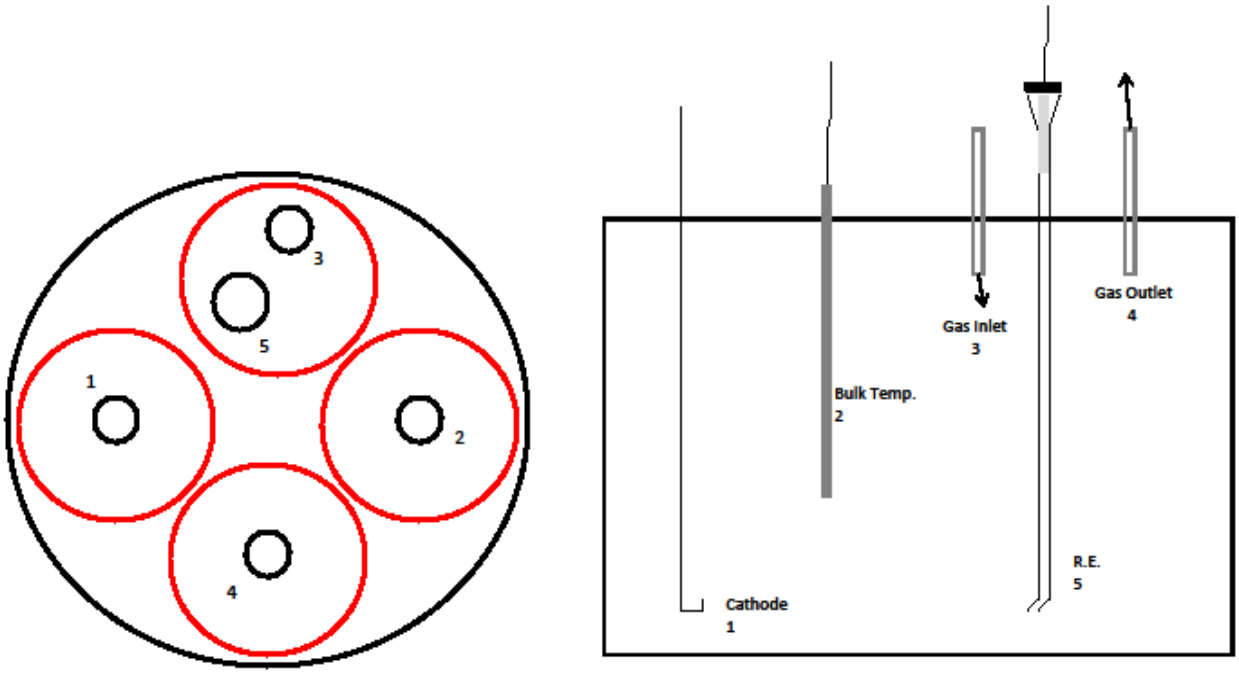

Figure 7. Top and side view of cathodic cell.

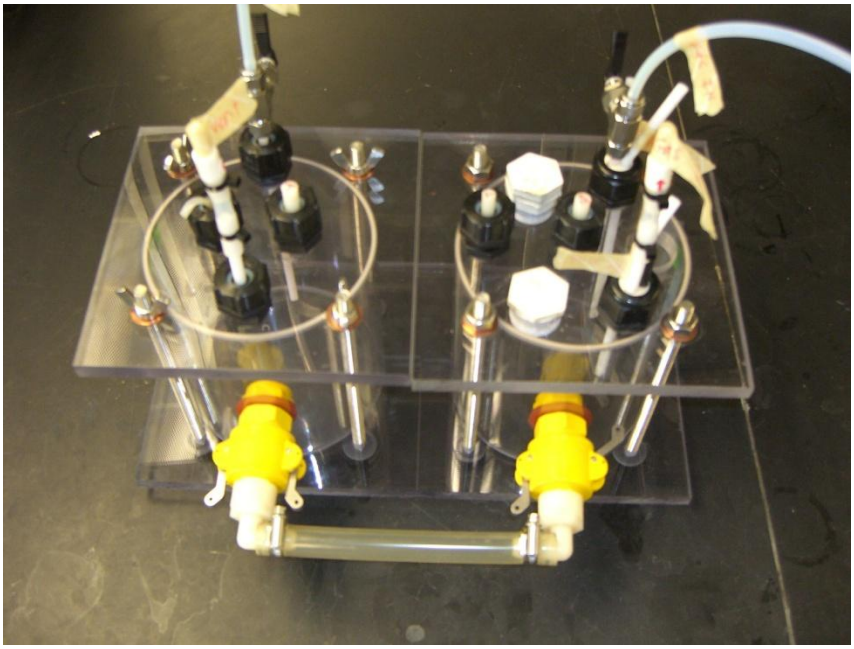

Figure 8. The assembled two-cell electrochemical system.

Electrochemistry and data acquisition

Figure 9 illustrates the setup and connections of electrochemical cells (anodic and cathodic cells) and the design of the electrochemical experiments for data collection. Three working electrodes (WE, anodes A1, A2, and A3) are immersed in AGM and bacteria culture in Cell A. The cathode coil is exposed to growth medium in Cell B without bacteria. An Ultra M micro Combination pH probe (model PHR-146B, Lazar Res Lab) is placed in close proximity to the surface of the A1 and A3 anodes to monitor the pH changes in the biofilm/metal interface. In addition, two Calomel reference electrodes (RE) are placed in close proximity to A3 and between A1 and A2 through the Reference Electrodes Bridge Tube. Cell A also contains a Graphite Counter Electrode (CE), a RE, and a pH probe for monitoring of pH of the bulk growth medium. Cell A and B are connected with a Salt Bridge filled with artificial growth medium and separated with a hydrophilic PVDF membrane filter (0.1 µm pore size) to prevent migration of bacteria from Cell A to Cell B.

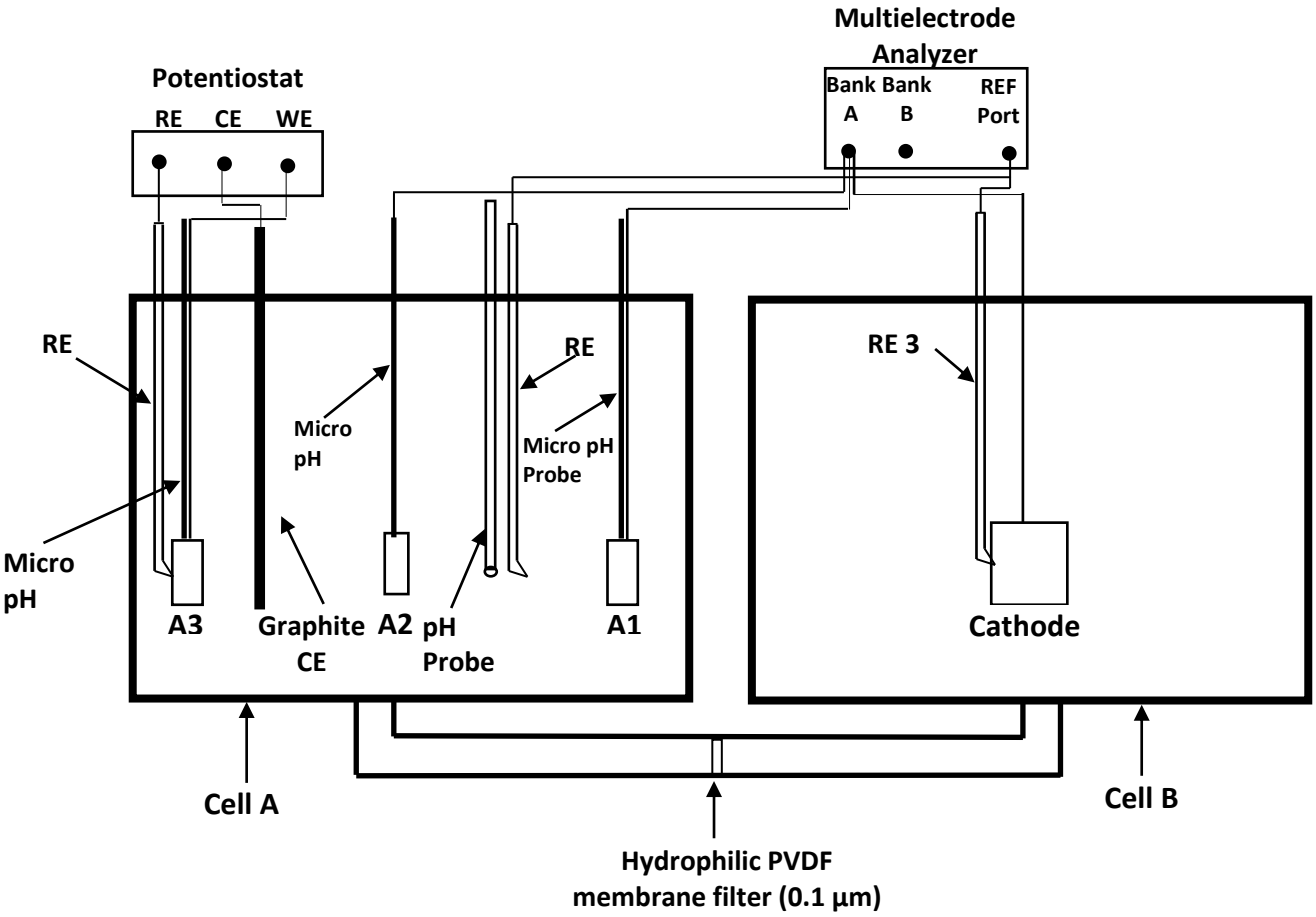

Figure 9. Setup and connections of electrochemical cells.

The small anode and large cathode electrodes are submerged under artificial growth medium in Cell A and B, respectively. Cell A is inoculated with an appropriate quantity of bacteria consortium and Cell B is abiotic. Anodes A1 and A2 are connected to the cathode through a Nano Corr S-18 Coupled Multielectrode Analyzer (Corr Instruments) for measurement of

electrode potential and coupling galvanic current between the anode and cathode using CorrVisual software at 1-hour intervals. While A2 is constantly connected, A1 will be disconnected from the Analyzer twice a day and connected to CE through a potentiostat/galvanostat/ZRA (Gamry Instruments Reference 600) for measurement of corrosion rate on anodes by linear polarization without the influence of galvanic current (A1-RE-CE connection). The corrosion rate of A3 is measured by potentiostat/galvanostat/ZRA before and after the corrosion rate measurement of A1. Unlike A1, A3 will never be connected to a large cathode; therefore, the corrosion rate of A3 (as control) is expected to be significantly lower than that of A1.

Test Protocol for Electrochemical Measurement of Microbial Corrosion

Sterilization and assembly of electrochemical cells

The electrochemical cells consist of many components, and some of them cannot be autoclaved. Sterilization of this two-cell system proved to be very challenging. The detailed sterilization of various parts and assembly procedures are summarized as following (reference to Figure 5, Figure 6, Figure 7, and Figure 8).

SSDS sterilization: The following components were sonicated for 5 min at the highest power, soaked in Sporicidin® Sterilizing and Disinfecting Solution (SSDS) overnight, deactivated with sterile 2% (w/v) glycol and 0.5% Tween 80 solution, and rinsed well with sterile di H_2O.

1) 3 micro pH probes (port a2, b2, and c2), bulk temperature probe (port 6), and bulk pH probe (port 5) in Anode cell
2) Bulk temperature probe (port 2) in Cathode cell
3) Various tubes in the cells

Autoclave sterilization (*at 121°C for 45 minutes)*

1) Dissemble the top and bottom plates and yellow connectors, autoclave the plates, bottle, seal, and yellow connector. Re-assemble.
2) Assemble anode cell for autoclave
    a. Attach plugged fitting for port 5 and 6.
    b. Attach 3 assembled fittings for port a, b, and c
        i. Plug port a2, b2, and c2 for micro pH probes
        ii. Fit a3, b3, and c3 for RE bridges without RE itself. Cap the empty bridge
        iii. Fit a1, b1, and c1 for WE
    c. Attach assembled fittings for 10, 8, 4 (media circulation, gas outlet, and CE)
    d. Attach assembled fittings for 7, 9, 11 (gas inlet, inoculation, and media circulation).
        i. Leave port 9 unplugged
        ii. Connect port 10 and 11 with tubing in order to seal
        iii. Plug port 7
3) Assemble cathode cell for autoclave
    a. Fit port 1 for cathode coil
    b. Attach plugged fitting for port 2 (bulk temp probe)
    c. Attached assembled fittings for ports 3 and 4 (gas inlet and outlet).
4) Place a 0.1-µm liquid filter into salt bridge and attach salt bridge to both cells

5) Connect cathode port 4 and anode port 8 with tubing, a T adapter and a pressure relief valve
6) Purge both cells with helium for five minutes at low pressure (100 kpa) with gas flow from cathode port 3 to anode port 9
7) Attach pressure gauge to anode port 9 and perform a pressure test
8) Remove pressure gauge and plug port 9
9) Prior to autoclave cover all ports with aluminum foil
10) Along with cell setup, autoclave length of tubing for ports connection

System assembly

1) Bring system over to the hood to cool down.
2) Attach various tubings and 0.2-μm filter disc for protection.
3) Pump in 2 L of media through media filter using anode port 11 and cathode port. Use T adaptor to release the pressure during media pumping.
4) Make sure the bridge tube is full of medium with no air bubbles.
5) Tighten all fittings
6) Autoclave again with medium in the cells

Anode wire and cathode coil sterilization and final assembly

1) Anode and cathode (C1018 carbon steel) are wet polished using silicon carbide (SiC) paper in sequence from 240-grit to 600-grit
2) Prior to use, wash with acetone, air-dry, and assemble immediately with fittings
3) Attach temperature probes (port 6) and micro pH probes (a2, b2, and c2), and bulk pH probe (port 5) to anode cell.
4) Attach temperature probe (port 2) to cathode cell
5) Heat-shrink tubing around micro pH probes to seal ports.

Test protocol

Anodes and cathode: The three anodes and one cathode coil are immersed in cell A (containing bacteria) and cell B (no bacteria), respectively. The surface area of the cathode is about 150:1 ratio to Anode A1 and A2 combined. A1 and A2 are connected to the cathode through the Multielectrode Analyzer. Anode A3 does not connect to the cathode; it is used for corrosion rate measurements with the Potentiostat.

Actual B value determination: The Stern-Geary Constant (B value) is made up of the anodic and cathodic Tafel slopes, and is generally accepted as a constant between 0.02 and 0.08 for a variety of steels under different environments. The default B value from the manufacturers of electrochemical corrosion monitoring device is usually around 0.030 V. However, past research [13, 15] has indicated significant difference between the default B values and actual B values measured by the electrochemical instrument. This is especially significant in a microbial corrosion system. Generally, the initial B values in a microbial system were close to the default value, and as the experiments went on, the B values decreased gradually, and then stabilized at a lower value in most cases. In this project, we used an InterCorr SmartCET electrochemical instrument to determine the actual B value under the conditions which are used in later corrosion modeling experiments. The average B value obtained from this experiment will be used for the

future corrosion modeling experiments to correct linear polarization corrosion rate (LPR) measured by the Potentiostat.

InterCorr C1018 probes were sonicated probes in ethanol (200-proof) for 1 min, degreased with acetone for 10 min, wrapped with sterile aluminum foil and dried in 60 ºC oven until use. InterCorr probe holders were soaked in SSDS overnight, deactivated, rinsed with sterile water, wrapped with sterile aluminum foil and dried in 60 ºC oven until use. Assembled bacteria culturing system incorporated with InterCorr SmartCET containing 200 mL of sterile AGM supplemented with 0.3% of NB medium was purged with filtered 94.3% N_2-5% H_2-0.7% O_2 gas mix for 60 minutes (

Figure **10**). The headspace of the culture container was purged with the gas mix daily to maintain a 0.7% oxygen condition after the experiment started. The bacteria consortium inoculum was prepared by mixing *B. licheniformis* at 6.0 x 10^6/ml and field enrichment culture at 6.0 x 10^7/ml at 1:1 ratio, washing once in PBS (pH 7.0), and resuspending in 1X AGM+0.3% NB medium. The culture container was inoculated with 10% bacterial consortium mix and incubated at 30 ºC. The result of the actual B value measurement is shown in

Figure **11**. As predicted, the actual B values varied significantly in the first few days of the experiment, and then became stabilized at lower level than default value. The typical B values after stabilization was calculated, as suggested by the inventors of InterCorr SmartCET [15], and will be used for the Potentiostat to measure the corrosion rate under the exposure to microbial consortium. The actual B value for the simulated system in this project was 0.01661.

Figure 10. Anaerobic bacteria culturing system incorporated with InterCorr SmartCET electrochemical device for real-time corrosion monitoring

Modeling parameter measurement: The following parameters are taken in electrochemical corrosion experiments for the purpose of MIC modeling.

1) Potential of A1 (or A2), and cathode is monitored using the Multielectrode Analyzer. The connection is as following: A1 (or A2) to Bank A of the Analyzer; cathode to Bank B of the Analyzer; RE1 in cell A, joined with RE3 of Cathode, and connects to RE connector

on the Analyzer.

2) Current flow of A1, A2, and Cathode is monitored using the Multielectrode Analyzer. The connection is as following: A1, A2 and cathode to Bank A; RE1 in cell A, joined with RE3 of Cathode, and connects to RE connector on the Analyzer.
3) Linear polarization corrosion rate (LPR) is measured using the Potentiostat with average of actual B value (0.01661) determined in the previous experiment.
    a. LPR of A1 is measured twice a day by disconnecting anode A1 from the Analyzer and then connecting A1, RE1, and CE to the Potentiostat.
    b. LPR of A3 is measured by connecting anode A3, RE2, and CE to the Potentiostat. The measurements of A3 take place before measurement for A1.
4) pH of the anode surface is measured using Ultra M micro combination pH electrode Model PHR-146B (Lazar Research Laboratories, Los Angeles, CA).The pH of bulk culture is also monitored.

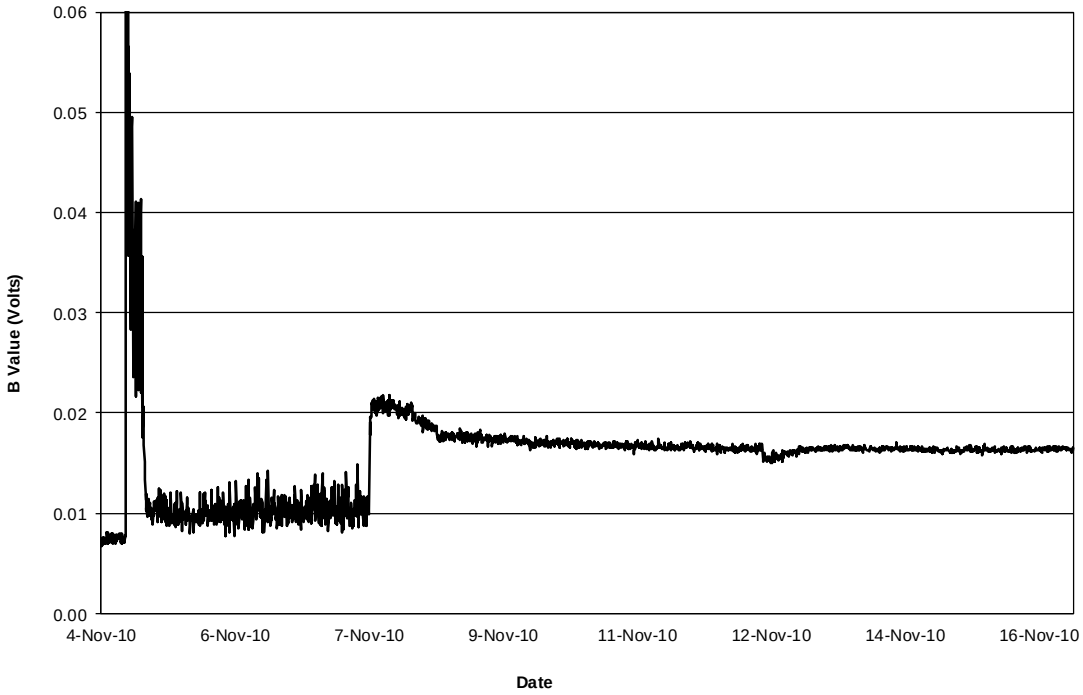

Figure 11. Actual B value determined by InterCorr SmartCET Instrument

Test protocol for electrochemical measurement of microbial corrosion: The two-electrochemical-cell system was set up according to 0. Both Cell A and B contain 2 L of sterile AGM supplemented with 0.3% of NB purged with filtered 94.3% N2-5% H2-0.7% O2 gas mix for 60 minutes. Cell A is inoculated with bacterial consortium, while Cell B is kept abiotic (see description in ***Actual B value determination*****)**. A salt bridge filled with same growth medium connects Cell A and B, but a hydrophilic PVDF membrane filter (0.1 µm pore size) in the bridge prevents the migration of bacteria from Cell A to Cell B. The temperatures of Cell A and B are maintained at 30 ºC with heating tape. In addition, the headspace of Cell A is purged with gas mix daily to maintain 0.7% oxygen condition.

After inoculation of bacteria consortium into Cell A, the experiment is operated as a batch cell and a daily culture sample is taken to determine the concentration of planktonic bacteria using the plate count method with serial dilution in triplicate. When the concentration reaches 10^6 cells/ml, medium replacement in Cell A starts. 10% of culture volume in Cell A is replaced daily with fresh growth medium filtered through a 0.2-µm membrane. The medium in Cell A is circulated at the rate of 2 L/day from bottom to top to avoid stratification. The medium composition in Cell A is analyzed periodically.

The potential of Cell A is measured by connecting anode A1 to bank A of the Multielectrode Analyzer and RE1 to REF port in the Analyzer (Figure 12). The potential of Cell B is measured by connecting cathode to bank B of the Multielectrode Analyzer and RE3 to REF port in the Analyzer (Figure 12). When a 10 mv difference between the two cells is reached, the difference is verified by connecting anode A2 to bank A in place of A1. The measured potential should be equal to the potential measured by connecting A1 (Figure 13). After the10 mv potential difference between the two cells is verified, the current between anodes (A1 and A2) and cathode will be measured by Multielectrode Analyzer, and the corrosion rate (LPR) of anode A3 and A1 will be measured by the Potentiostat by making the connections illustrated in

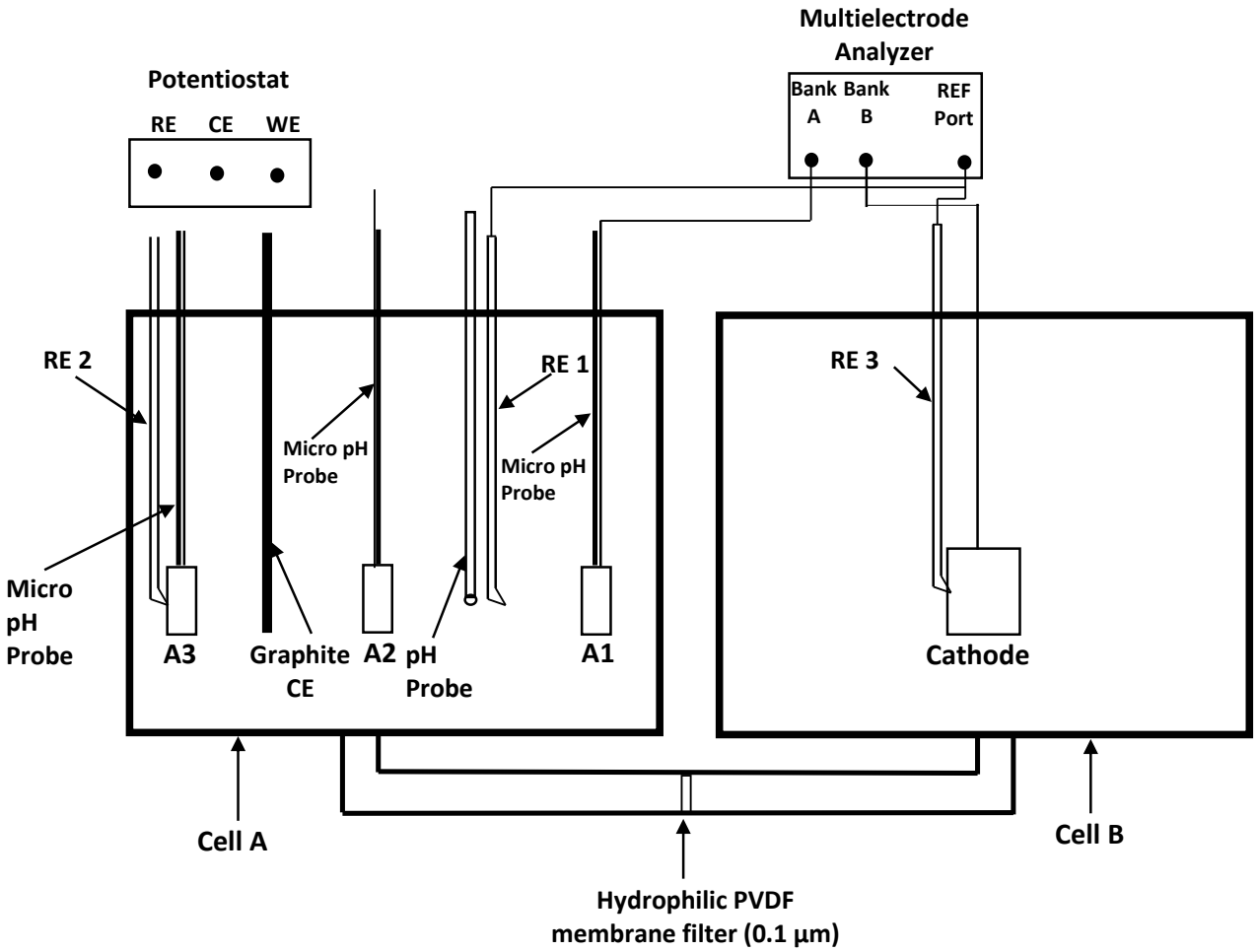

Figure 14.

Figure 12. Electrochemical test setup to monitor potential difference between anode and cathode.

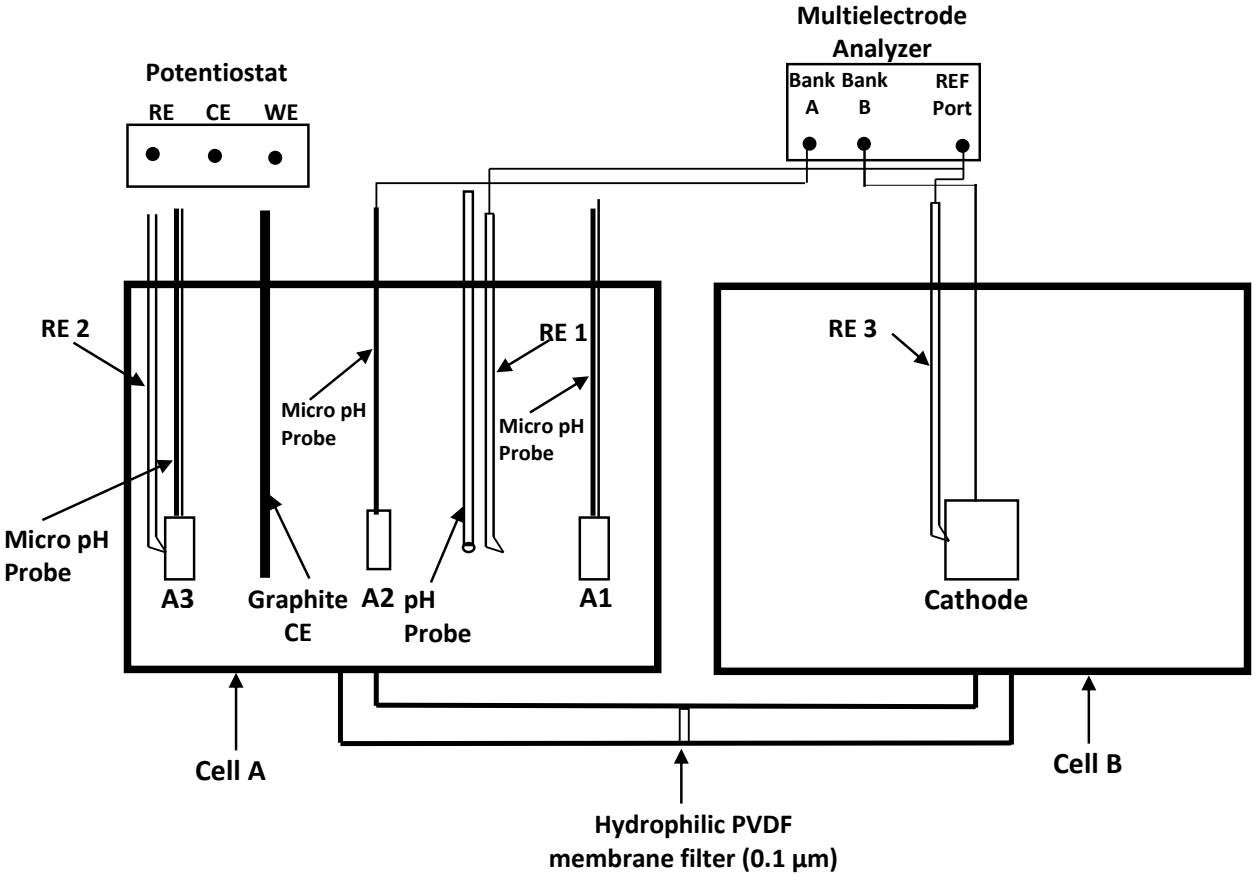

Figure 13. Electrochemical test setup to verify potential difference between A1 and A2.

The current between anodes (A1 and A2) and cathode is monitored by connecting A1, A2 and cathode to Bank A in Multielectrode Analyzer, and joining RE1 and RE3 and then connecting to REF port of the Analyzer (

Figure 14). The corrosion rate (LPR) of anode A3 is measured twice a day by connecting CE, A3 and RE2 to the Potentiostat (

Figure 14). The corrosion rate (LPR) of anode A1 is measured by connecting CE, A1 and RE1 to the Potentiostat. The measurements of A1 corrosion rate are performed twice a day after temporarily disconnected from the Analyzer and connected to the Potentiostat. pH close to the anode surface is measured by the Analyzer using micro pH probe.

The electrochemical data and other data (e.g pH, chemical composition of medium) will be used to develop a preliminary model for prediction of corrosion rate under the influence of the bacteria consortium. At the end of the experiment, the anode will be fixed with 2% glutaraldehyde buffered with 0.2 M sodium phosphate for 12 hours, dehydrated in acetone-distilled water series of 25%, 50%, 80%, and 100% acetone (10 minutes each), dried at 80 ºC for 10 minutes, and placed in a desiccator until inspection. The inspection will include scanning electron microscope (SEM) for determination of the biofilm thickness and structure, pit shape and diameter, and EDS/EDX and Raman Spectroscopy for pit chemistry.

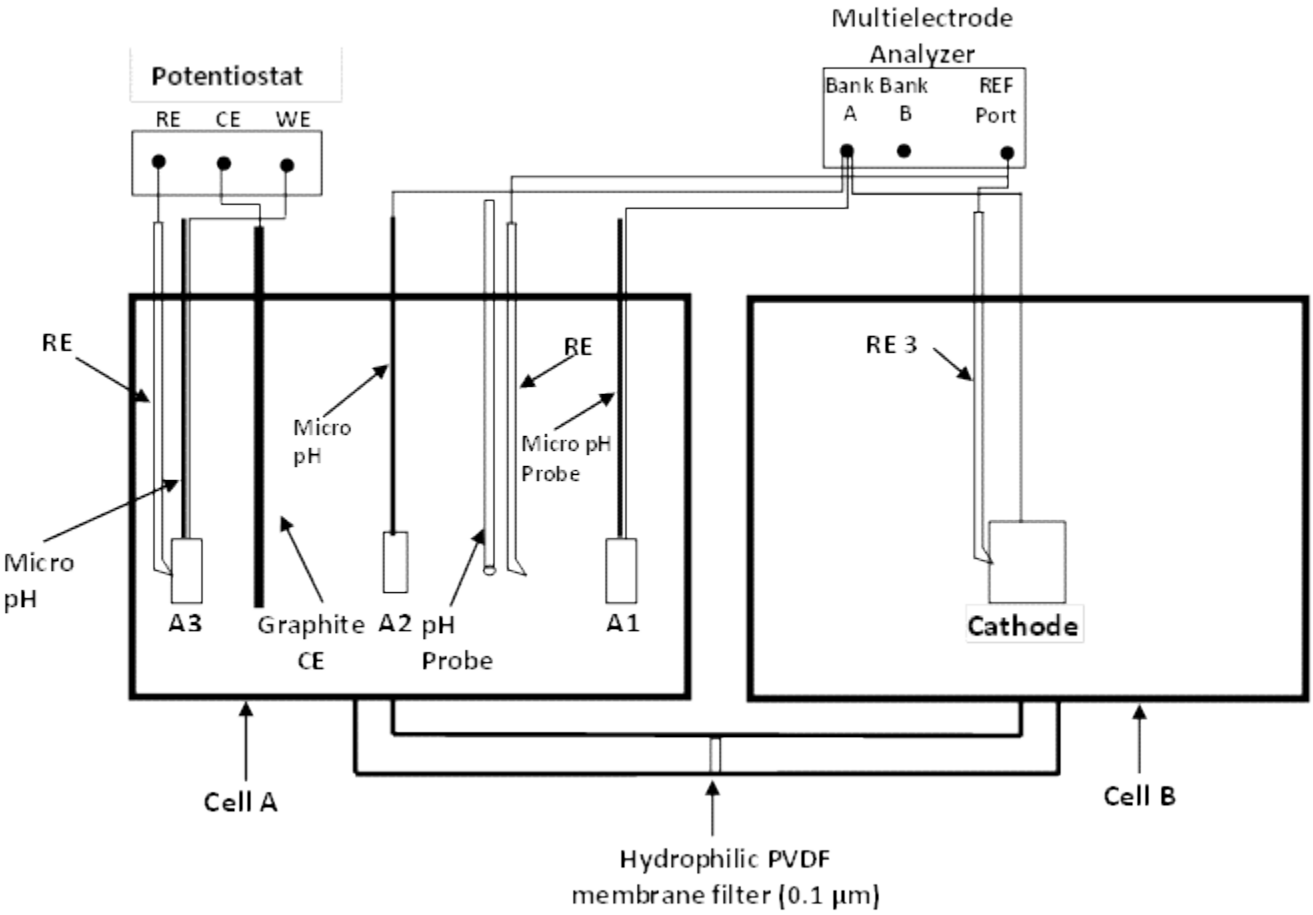

Figure 14. Electrochemical test cell setup for current and corrosion rate monitoring.

Task 8 - Perform Bounded Testing to Generate a Strong Example Data Set

The activities performed inTask 8 during this quarter include (a) developing a protocol for collecting the raw/processed biogas samples from the plants, (b) designing and building pressure test vessels for gas saturation testing, (c) identifing commercial plastic pipe and elastomer materials for testing, (d) identifying the sites to collect sample gases (raw landfill gas, processed landfill gas and raw dairy gas), and (e) obtaining test materials and gas samples.

A HazOp analysis has been completed in this quarter for the safety review on the gas sample collection process at the sites. A Baseline Hazard Analysis has also been completed for gas saturation

testing. The design of the pressure test vessel has been finalized and the construction of one test vessel and sample cage has been completed.

A commercial pipe grade MDPE (medium density polyethylene) resin was selected to be used for making the plastic test samples. The premium grade NBR (Butadiene Acrylonitrile) and SBR (Butadiene Styrene) sheet materials were selected to be used for making rubber test samples. The formulations and properties of the selected NBR and SBR sheet materials are close to the rubber materials used in natural gas pipeline systems. The test materials have been ordered, and will be arrived by end of the year.

The natural gas sample has been selected to be used in this testing as a reference gas to evaluate the impact on material properties by biogas/biomethane. It reflects a gas quality typical to tariffs imposed by LDCs located in the Midwest.

Protocol for Biogas Collection

The biogas samples will be collected from biogas plants and compressed into a high pressure cylinder (lowered to 1800 psi from 2000 psi) and returned to GTI in order to supply the gas for the saturation tests. The raw biogas supplied in the plant is near ambient pressure, and it has to be compressed by a compressor so that it can be filled into the high pressure gas cylinder. A portable compressor (FuelMaker FM4) which can be brought to the sample collection sites is being modified for this use at GTI.

The raw biogas is generally saturated with moisture and the liquid water will be condensate from the gas at high pressure when the gas is compressed. Some compounds in the raw gas may dissolve in the water condensate and result in the variation of the gas composition. To avoid this change of gas chemistry during sample collection, the raw gas will be dehydrated before it is compressed.

FuelMaker FM4 Compressor

The specification for the compressor to be used to collect biogas samples has been developed, and it is shown in Figure 15. The unit selected is the FuelMaker FM4 compressor, with a power requirement of 220 Volts, 1 phase AC (at 60 Hz). It draws 6 Amps of current, resulting in an average electrical consumption between 0.9-1.3 kWh.

Considerations for Gas Sampling at Biogas Plants

1) Determine the following site specifications:
    - Electrical power on-site (e.g. 240 Volts)
    - Pipe fittings from site gas outlet
    - Gas pressure from site gas outlet
    - Pipe fittings for processed biomethane (if applicable)
    - Gas pressure for processed biomethane (if applicable)
2) The sampling schematic will be configured as shown in Figure 15.
3) A HazOp analysis will be performed on this process to ensure the safety and quality of our process.
4) Properties to consider when collecting gas are the following:
    - Temperature of gas (50°C-60°C).
    - Density change during compression (for compressibility factor).
    - Impurities that may affect equipment (H_2S, siloxanes, etc.).

- Liquid condensation by dew-point from components (e.g. CO_2).

Biogas/Biomethane Gas Sample Sites

The biogas/biomethane gas sample sites have been selected from the gas sample database at GTI. These include a landfill site where the raw and processed landfill gas samples will be collected and a dairy farm site where the raw dairy gas sample will be collected. The compositions of the biogas/biomethane gases from these sites are representative to the gases that have been analyzed at GTI.

Gas Saturation Test Setup

The test samples will be saturated in the sample gases including one natural gas (as reference), one raw landfill gas, one processed landfill gas (biomethane) and one raw dairy gas. The gas saturation will be performed at ~ 45ºC to simulate the worse scenario in the biogas gathering line where biogas is delivered out of the digester.

The gas saturation test setup is shown in Figure 16. A stainless steel pipe is used to make the pressure vessel as the chamber for the gas saturation test. The test samples will be loaded onto a sample cage made of stainless steel mesh to allow the test samples to be fully exposed to the gas, see Figure 17. The vessel will then be purged with the tested gas before the test is started. A low gas flow will be maintained during the saturation test (0.05 cc/min).

The pressure test vessel has been designed for the gas saturation test, see Figure 18. It consists of a three feet long and four inch diameter stainless steel (SS316) pipe. The pipe will be heated with the heat tape wrapped around the outer surface of the pipe, and the temperature inside the pipe will be maintained at 45±5ºC by a temperatuare controlling system.

Test Materials

NBR and SBR Rubber Sheet Materials

A sheet rubber material was decided to be used for the testing in order to prepare the samples with a standard sample size. This will reduce the data scatter resulted from sample variation and improve the comparative test results for a better evaluation of the impact from biogas/biomethane. GTI has reviewed the NBR and SBR materials that are most used in natural gas pipeline, and selected the rubber sheet materials that have closer physical and chemical properties, see Table 4. The test samples will be die cut from the sheet materials.

Natual Gas Sample

A standard natural gas was selected for the saturation test as a reference to compare the impact from biogas/biomethane on the pipeline materials. The approximate chemical compositions of the natural gas sample is shown in Table 5. A full analysis will be performed to obtain actual compositions.

Biogas/Biomethane Samples

Sites have been selected to collect processed biomethane from landfill, raw landfill biogas, and raw dairy farm biogas. The approximate chemical compositions of the natural gas sample is shown in Table 5. These values were obtained from GTI's database of the selected sites. A full analysis will be performed to obtain actual compositions on each of the gases.

Table 4. The Properties of NBR and SBR Rubber Sheet Mateirals

Rubber Sheet	Hardness (Shore A)	Tensile (psi)	Ultimate Elongation (%)	Heat Aging	Oil Resistance	Temperature Range
NBR	70	1500 min	250 min	(70 hrs @ 100ºC) Hardness: ±15 points Tensile: ±30% max Elongation: -50% max	(70 hrs @ 100ºC) Hardness: -10 to +5 points Tensile: -45% max Elongation: -45% max Volume: 0 to 25% max	-40º to 200ºF
SBR	65	1000 min	250 min	(94 hrs @ 100ºC) Hardness: 10 points max Tensile: -20% max Elongation: -35% max	NA	NA

Table 5. Chemical Compositions (approximate) of Gas Samples

Gas Property	Natural Gas	Raw Dairy Farm Gas	Raw Landfill Gas	Processed Biomethane
Methane (CH_4)	90%	62%	55%	97%
Carbon Dioxide (CO_2)	2 – 3% Maximum	35%	32%	BDL
Nitrogen (N_2)	3% Maximum	2%	11%	2%
Helium (He)	0.2% Maximum	BDL	BDL	BDL
Mercury (Hg)	BDL	0.06 µg/m^3	0.06 µg/m^3	BDL
Oxygen (O_2)	0.2% Maximum	0.4%	1.0%	BDL
Hydrogen Sulfide (H_2S)	Less than 1 grain for every 100scf (approx. 15 ppmv)	4,225 ppmv	137 ppmv	BDL

Note: Concentrations are in mol %, unless specified otherwise. Natural Gas quantities are based on LDC tariffs. BDL denotes quantities below the detection limits of the instrumentation used for analysis.

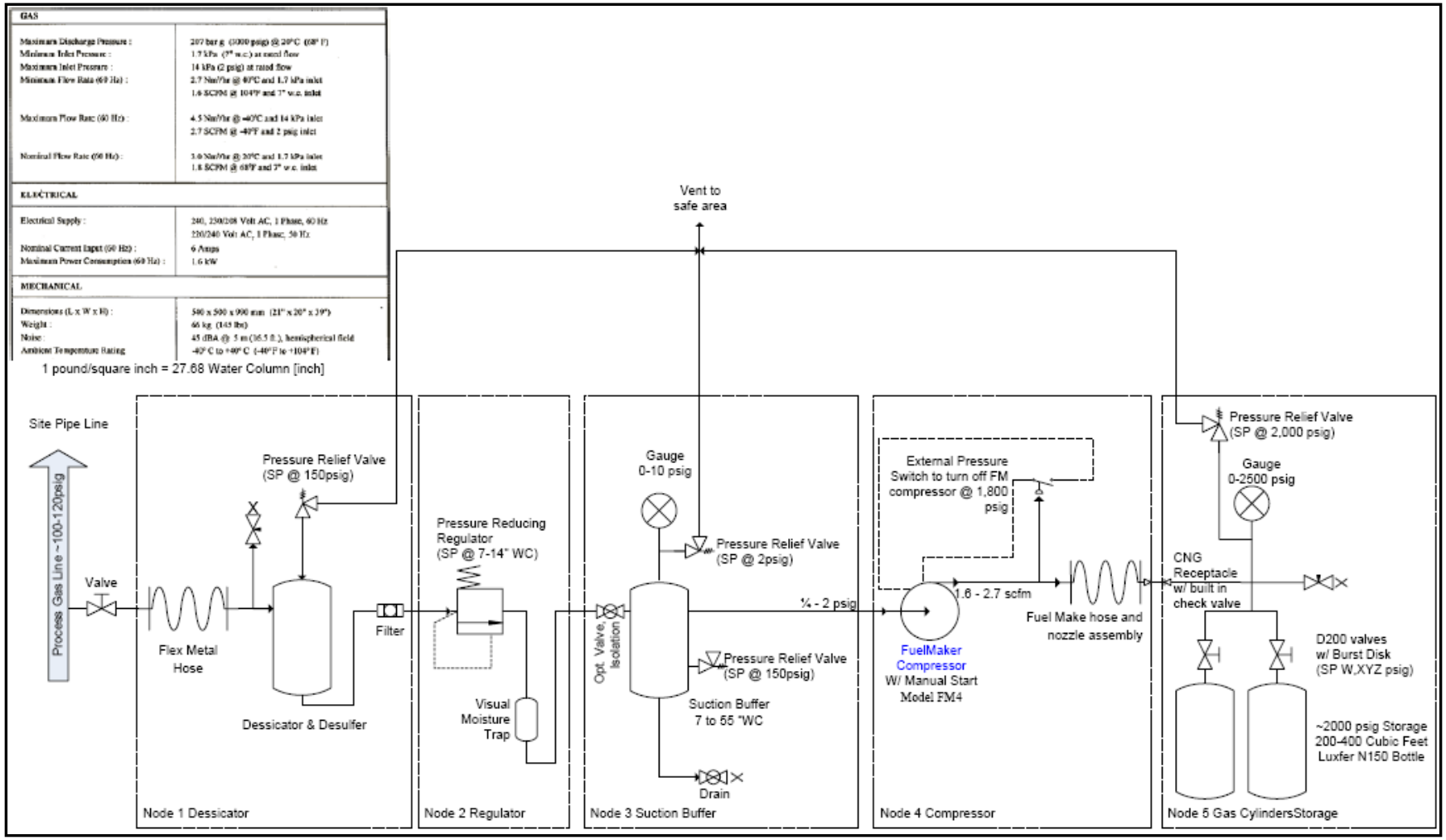

Figure 15. Biogas Collection Schematic (Updated)

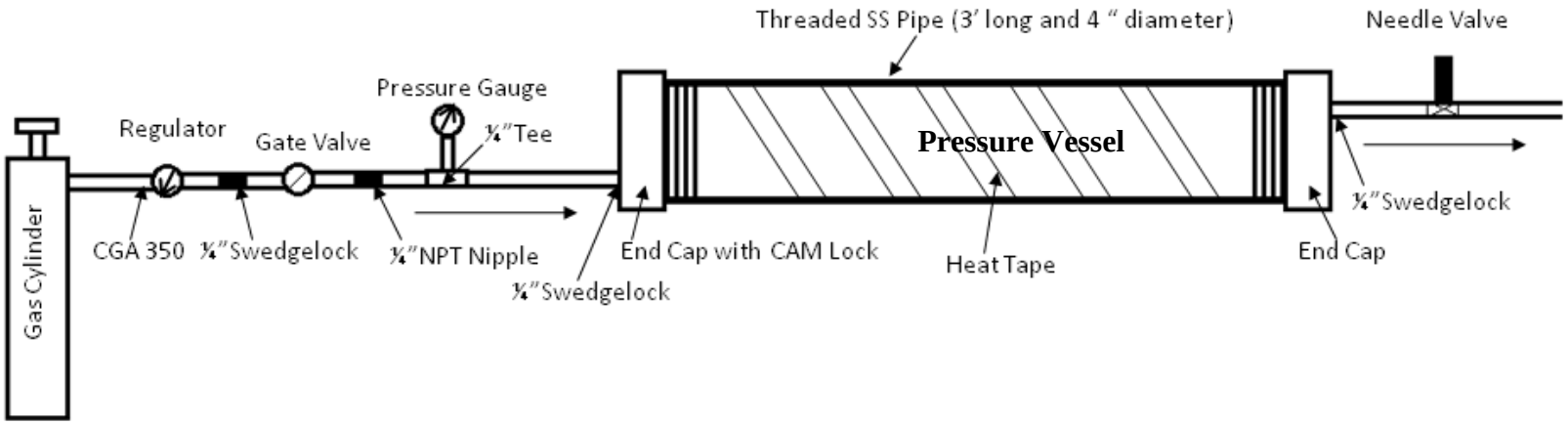

Figure 16. Gas Saturation Test Setup

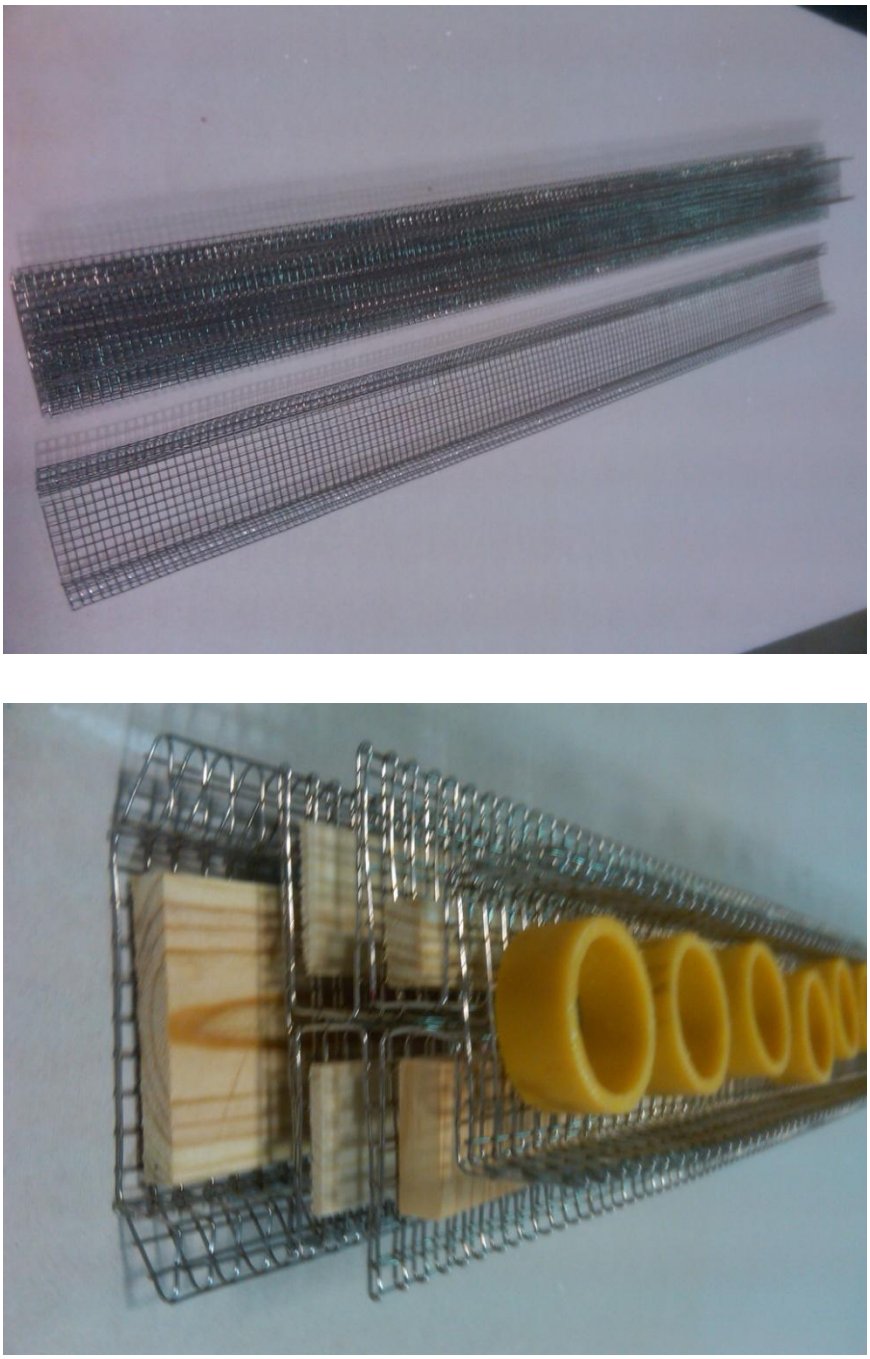

Figure 17. Test Sample Cage

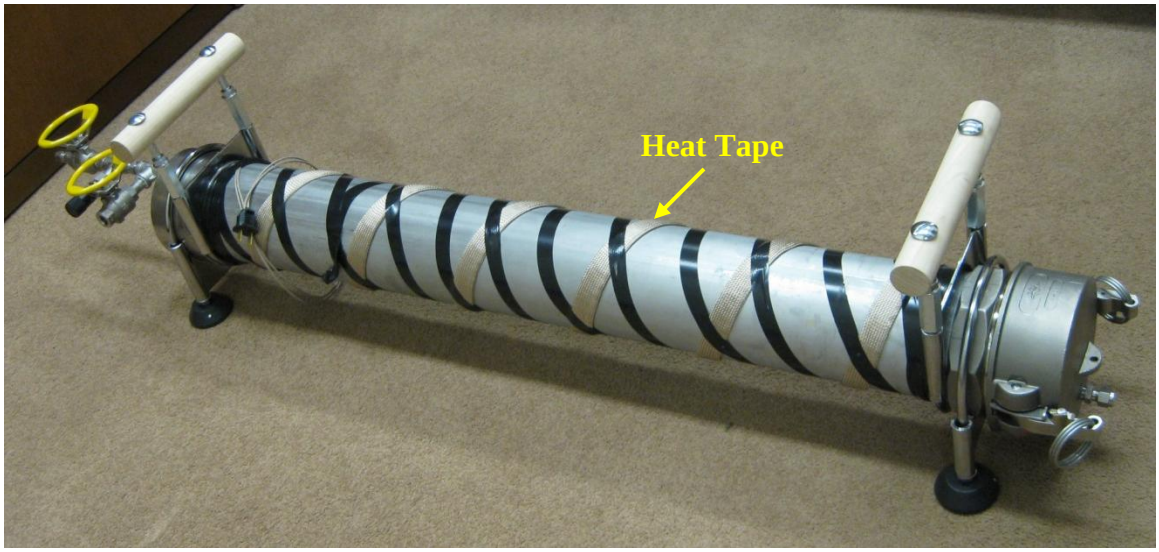

Figure 18. Pressure Vessel for Gas Saturation Test

References

1. Angostini, R.A. and R.D. Young, *A case history: Investigations of microbially influenced corrosion in a west Texas waterflood. NACE paper no. 119.* 1990.
2. Farthing, S., *Company combats MIC with aggressive control program.* Pipeline and Gas Industry, 1997. **Oct '97**: p. 43-47.
3. Pope, D.H. and R.M. Pope, *Guide for the Monitoring and Treatment of Microbiologically Influenced Corrosion in the Natural Gas Industry*. 1998, Gas Research Institute.
4. Pope, D.H., et al., *Mitigation strategies for microbially influenced corrosion in gas industry facilities.* Corrosion '89, 1989: p. NACE paper 192.
5. Strickland, L.N., R. T. Fortnum, B. W. DuBose, *A case history of microbiologically influenced corrosion in the Lost Hills oilfield, Kern county California.* Corrosion '96, 1996: p. NACE paper 297.
6. Emde, K.M.E., D. W. Smith, and R. Facey, *Initial investigation of microbially influenced corrosion (MIC) in a low temperature water distribution system.* Water Research, 1992. **26**: p. 169-175.
7. Angell, P., *Understanding microbially influenced corrosion as biofilm-mediated changes in surface chemistry.* Curr. Opin. Biotechnol., 1999. **10**(3): p. 269-72.
8. Dzierzewicz, Z., B. Cwalina, L. Weglarz, S. Glab, *Isolation and evaluation of corrosive aggressivity of wild strains of sulfate reducing bacteria.* Acta Microbiologica Polonica, 1992. **41**: p. 211-221.
9. Dzierzewicz, Z., et al., *The relationship between microbial metabolic activity and biocorrosion of carbon steel.* Res. Microbiol., 1997. **148**(9): p. 785-93.
10. Hamilton, W.A., *Sulphate-reducing bacteria and anaerobic corrosion.* Annu. Rev. Microbiol., 1985. **39**: p. 195-217.
11. Horn, J. and D. Jones, *Microbiologically influenced corrosion: Perspectives and approaches*, in *Manual of environmental microbiology*, C.J. Hurst, Crawford, R. L., Knudsen, G. R., McInerney, M. J., Stetzenbach, L. D., Editor. 2002, ASM Press: Washinton, DC. p. 1072-1083.
12. Zhu, X.Y., *"Detection and Mitigation of Microbiologically-Influenced Corrosion (MIC) in Natural Gas Pipelines". GTI Project 20153, completed in March 2007.* 2007.
13. Zhu, X.Y., H. Modi, and J.J. Kilbane II, *Efficacy and risks of nitrate application for the mitigation of SRB-induced corrosion.* In Proceedings of the NACE International Annual Conference, Corrosion/2006, Paper #06524. San Diego, CA., 2006: p. 1-41.
14. Li, S.Y., et al., *Microbiologically Influenced Corrosion of Carbon Steel Exposed to Anaerobic Soil.* Corrosion, 2001. **57**(9): p. 815-828.
15. Kane, R.D. and S. Campbell, *Real-Time Corrosion Monitoring of Steel Influenced by Microbial Activity (SRB) in Simulated Seawater Injection Environments.* CORROSION NACExpo'04, 2004: p. NACE Paper 04579.
16. King, R.A. and D.S. Wakerley, *Corrosion of Mild Steel by Ferrous Sulphide.* Br Corros J, 1973. **8**(1): p. 41-45.
17. King, R.A., J.D.A. Miller, and D.S. Wakerley, *Corrosion of Mild Steel in Cultures of Sulphate-Reducing Bacteria: Effect of changing the soluble iron concentration during growth.* Br Corros J, 1973. **8**(2): p. 89-93.

18. Jack, T.R., et al., *Corrosion Consequences of Secondary Oxidation of Microbial Corrosion.* Corrosion, 1998. **54**(3): p. 246-252.

19. Zhu, X.Y., *"Bioreactor/Chemostat System for Rapid Biodemilitarization of Munitions" for DOD/DARPA, subcontracted from SRI. Subcontract No. 41-000810. GTI project No. 20569. Completed in Angust 2008.*

20. de Franca, F.P. and M.T.S. Lutterbach, *Variation in sessile microflora during biofilm formation on AISI-304 stainless steel coupons.* Journal of industrial microbiology, 1996. **17**(1): p. 6-10.

21. Pope, D.H. and R.M. Pope, *Microbiologically Influenced Corrosion in Fire Protection Sprinkler Systems*, in *A Practical Manual on Microbiologically Influenced Corrosion*, J.G.S. II, Editor. 2001, NACE International: Houston, TX. p. 5.1-5.7.

22. NACE, *Detection, Testing, and Evaluation of Microbiologically Influenced Corrosion (MIC) on External Surfaces of Buried Pipelines.* NACE Standard TM0106-2006, 2006.

23. Batista, J.F., R. F. Pereira, J. M. Lopes, M. F. Carvalho, M. J. Feio, M. A. Reis,, *In situ corrosion control in industrial water systems.* Biodegradation, 2000. **11**(6): p. 441-8.

24. Kasahara, K. and F. Kajiyama, *Role of Sulfate Reducing Bacteria in the Localized Corrosion of Buried Pipes.* Biologically Induced Corrosion; Proceedings of the International Conference on Biologically Induced Corrosion. June 10-12, 1985, Gaithersburg, Maryland. Houston, TX, NACE., 1986: p. 171-183.

25. Shi, X., R. Avci, and Z. Lewandowski, *Microbially deposited manganese and iron oxides on passive metals—their chemistry and consequences for material performance.* Corrosion, 2002. **58**: p. 728.

26. Waters, M.S., et al., *Simultaneous interferometric measurement of corrosive or demineralizing bacteria and their mineral interfaces.* Appl Environ Microbiol., 2009. **75**(5): p. 1445-1449.

27. Little, B.J., P.A. Wagner, and Z. Lewandowski, *The role of biomineralization in microbiologically influenced corrosion, p. 294/1–294/18. In Proceedings of the CORROSION/98 Research Topical Symposia. NACE International, Houston, TX.* 1998.

28. Pope, D.H., *Microbiologically Influenced Corrosion of Internal Aspects of Natural Gas Industry Pipelines and Associated Equipment: Mechniasms, Diagnosis, and Mitigation*, in *A Practical Manual on Microbiologically Influenced Corrosion*, J.G.S. II, Editor. 2001, NACE International: Houston, TX. p. 6.13-6.25.

29. Pope, D.H., et al., *Organic Acid Corrosion of Carbon Steel: A Mechanism of Microbiologically Influenced Corrosion.* In Proceedings of the NACE International Annual Conference, Corrosion/1988, Paper #79. Houston, TX., 1988.

30. Graves, J.W., E. H. Sullivan, *Internal corrosion in gas gathering systems and transmission lines.* Materials Protection, 1996. **5**: p. 33-37.

31. Kholodenko, V.P., S. K. Jigletsova, V. A. Chugnov, V. B. Rodin, V. S. Kobelev, S. V. Karpov, *Chemicomicrobiological diagnostics of stress corrosion cracking of trunk pipelines.* Appl. Biochem. Microbiol., 2000. **36**: p. 594-601.

32. Pope, D.H., T. P. Zintel, B. A. Cookingham, R. G. Morris, D. Howard, R. A. Day, J. R. Frank, and G. E. Pogemiller, *Mitigation strategies for microbially influenced corrosion in gas industry facilities.* Corrosion '89, 1989: p. NACE paper 192.

33. Pope, D.H., R. M. Pope, *Guide for the monitoring and treatment of microbiologically influenced corrosion in the natural gas industry.* 1998, Gas Research Institute.

34. Scott, P.J.B., *Expert Consensus on MIC: Prevention and Monitoring.* Materials Performance, 2004(3): p. 2-6.

35. Jack, T.R., et al., *Microbiologically Influenced Corrosion Testing*, in *The Characterization of Sulfate-Reducing Bacteria in Heavy Oil Waterflood Operations*, J.R. Kearns and B.J. Little, Editors. 1994, Philadelphia, PA: ASTM. p. 108.

36. von Wolzogen Kuhr, C.A.H. and L.S. van der Vlugt, *The graphitization of cast iron as an electrochemical process in anaerobic soils.* Water Research, 1934. **18**: p. 147-165.

37. McNeil, M.B. and B.J. Little, *Mackinawite Formation During Microbial Corrosion,.* Corrosion, 1990. **46**: p. 599-600.

38. Tributsch, H., et al., *Role of Transient Iron Sulfide Films in Microbial Corrosion of Steel.* Corrosion, 1998. **54**(3): p. 216-227.

39. Hardy, J.A. and J.L. Brown, *The Corrosion of Mild Steel By Biogenic Sulfide Films Exposed to Air.* Corrosion, 1984. **40**(12): p. 650.

40. Jack, T.R. and M.J. Wilmott, *Indicator Minerals Formed During External Corrosion of Line Pipe.* MP, 1995. **34**: p. 19.

41. Pope, D.H. and E.A.M. III, *Some Experiences With Microbiologically Influenced Corrosion of Pipelines.* MP, 1995. **34**(5): p. 23.

42. Gibson, G.R. and X. Wang, *Regulatory effects of bifidobacteria on the growth of other colonic bacteria.* J. Appl. Bacteriol., 1994. **77**(4): p. 412-20.

43. Zellner, G., et al., *Anaerofilum pentosovorans gen. nov., sp. nov., and Anaerofilum agile sp. nov., two new, strictly anaerobic, mesophilic, acidogenic bacteria from anaerobic bioreactors.* Int. J. Syst. Bacteriol., 1996. **46**(4): p. 871-5.

44. Kanauchi, O., et al., *Increased growth of Bifidobacterium and Eubacterium by germinated barley foodstuff, accompanied by enhanced butyrate production in healthy volunteers.* Int. J. Mol. Med., 1999. **3**(2): p. 175-9.

45. Broda, D.M., et al., *Clostridium algidixylanolyticum sp. nov., a psychrotolerant, xylan- degrading, spore-forming bacterium.* Int. J. Syst. Evol. Microbiol., 2000. **50 Pt 2**: p. 623-31.

46. Vetting, M.W., et al., *Structure of Acinetobacter strain ADP1 protocatechuate 3, 4-dioxygenase at 2.2 A resolution: implications for the mechanism of an intradiol dioxygenase.* Biochemistry, 2000. **39**(27): p. 7943-55.

47. Zhu, X.Y., J. Lubeck, and J.J. Kilbane, 2nd, *Characterization of microbial communities in gas industry pipelines.* Appl Environ Microbiol, 2003. **69**(9): p. 5354-63.

48. Little, B.J. and P. Wagner, *Microbiologically Influenced Corrosion*, in *Peabody's Control of Pipeline Corrosion*, R.L. Bianchetti, Editor. 2001, Houston, TX: NACE, 2001.

49. Towers, R., *Accelerated Corrosion in Cargo Tanks of Large, Double-Hull Ships, Causes and Countermeasures.* Protective Coatings Europe, 2000(3): p. 30-42.

50. Hines, M.E., P.T. Visscher, and R. Devereux, *Sulfur cycling*, in *Manual of Environmental Microbiology*, L.D. Stetzenbach, Editor. 2002, ASM Press: Washington, DC. p. 427-438.

51. Mudryk, Z.J., et al., *The occurrence and activity of sulphate-reducing bacteria in the bottom sediments of the Gulf of Gdañsk.* OCEANOLOGIA, 2000. **42**(1): p. 105-117.

52. Caumette, P., *Ecology and physiology of phototrophic bacteria and sulphate-reducing bacteria in marine salterns.* Experientia, 1993. **49**: p. 473-481.

53. Bak, F. and P. N., *Sulfate-reducing bacteria in littoral sediment of Lake Constance.* FEMS Microbiol. Ecol., 1991. **85**: p. 43–52.

54. Le Borgne, S., et al., *Detecting and Monitoring Bacteria in Seawater Injection Systems.* Materials Performance, 2007. **46**(11): p. 52-56.

55. Jack, T.R., *MIC in Underground Environments: External Corrosion in the Gas pipeline Industry*, in *A Practical Manual on Microbiologically Influenced Corrosion*, J.G.S. II, Editor. 2001, NACE International: Houston, TX. p. 6.1-6.42.

56. Campaignolle, X., et al., *Stabilization of Localized Corrosion of Carbon Steel by Sulfate-Reducing Bacteria.* Nace International Corrosion 93, Paper no. 302, 1993: p. 1-7.

57. Daumas, S., M. Magot, and J.L. Crolet, *Measurement of the net production of acidity by a sulphate-reducing bacterium: experimental checking of theoretical models of microbially influenced corrosion.* Res. Microbiol., 1993. **144**(4): p. 327-332.

58. Hemmingsen, T., H. Vangdal, and T. Våland, *Formation of Ferrous Sulfide Film from Sulfite on Steel Under Anaerobic Conditions.* Corrosion, 1992. **48**(6): p. 475-481.

59. Campaignolle, X. and J.-L. Crolet, *Method for Studying Stabilization of Localized Corrosion on Carbon Steel by Sulfate-Reducing Bacteria.* Corrosion, 1997. **53**(6).

60. Tanji, Y., et al., *Chemical Analysis of an Artificial Biofilm that Enhances or Inhibits Carbon Steel Corrosion.* Corrosion, 2002. **58**(3): p. 232-239.

61. King, L.D. and J.D.A. Miller, *Corrosion by the sulfate reducing bacteria.* Nature, 1971. **233**: p. 491-492.

62. King, R.A., J.D.A. Miller, and J.S. Smith, *Corrosion of mild steel by iron sulfides.* Brit Corrosion J, 1973. **8**: p. 137-142.

63. Angeles-Ch, C., et al., *Microbiologically Influenced Corrosion by Citrobacter in Sour Gas Pipelines.* Materials Performance, 2002. **41**(8): p. 50-55.

64. Little, B.J., R.I. Ray, and R.K. Pope, *Relationship Between Corrosion and the Biological Sulfur Cycle: A Review.* Corrosion, 2000. **56**(4): p. 433.

65. Gonzalez, J.L., et al., *A damage model for assessing pipeline safety in corrosion environments.* Corrosion, 1997. **53**: p. 935-943.

66. Zhu, X.Y., *Rapid Quantification of Butyric Acid-Producing Bacteria Using Real-Time PCR*. 2007, Gas Technology Institute: USA.

67. Zhu, X.Y., *Rapid Quantification of Acetic Acid-Producing Bacteria Using Real-Time PCR*. 2008, Gas Technology Institute: USA.

68. Emerson, D. and W.C. Ghiorse *Isolation, Cultural Maintenance, and Taxonomy of a Sheath-Forming Strain of Leptothrix discophora and Characterization of Manganese-Oxidizing Activity Associated with the Sheath.* Appl. Environ. Microbiol., 1992. **58**: p. 4001-4010.

69. Hanert, H.H., *The genus Siderocapsa (and other iron- or manganese-oxidizing eubacteria,* in *The Prokaryotes, a Handbook on Habitats, Isolation and Identification of Bacteria,* M. Starr, et al., Editors. 1981, Springer-Verlag: New York. p. 1049-1059.

70. Dickinson, W.H. and Z. Lewandowski, *Manganese Biofouling and the Corrosion Behavior of Stainless Steel.* Biofouling, 1996. **10**: p. 79-93.

71. Hamilton, W.A., *Sulphate-reducing bacteria and anaerobic corrosion.* Ann. Rev. Microbiol., 1985. **39**: p. 195-217.

72. Zhu, X.Y., et al., *Rapid detection and quantification of microbes related to microbiologically influenced corrosion using quantitative polymerase chain reaction.* Corrosion, 2006. **62**: p. 950-955.

73. Zhu, X.Y., et al., *Application of Quantitative, Real-Time PCR in Monitoring Microbiologically-Influenced Corrosion (MIC) in Gas Pipelines.* In Proceedings of the NACE International Annual Conference, Corrosion/2005, Paper #05493. Houston, TX., 2005: p. 1-20.

74. Myers, C. and K.H. Nealson, *Bacterial Manganese Reduction and Growth with Manganese Oxide as the Sole Electron Acceptor.* Science, 1988. **240**: p. 1319.

75. Dubey, R.S. and Upadhyay, *Microbial Corrosion Monitoring by an Amperometric Microbial Biosensor Developed using Whole Cell of Pseudomonas sp.* Biosensors and Bioelectronics, 2001. **16**: p. 995-1000.

76. Nordstrom, D.K. and G. Southam, *Geomicrobiology of Sulfide Mineral Oxidation*, in *Reviews in Mineralogy Geomicrobiology: Interactions Between Microbes and Minerals*, J.F. Banfield and K.H. Nealson, Editors. 1997, Washington, DC: Mineralogical Society of America. p. 361-390.

77. Boivin, J., et al., *The Influence of Enzyme Systems on MIC.* CORROSION/90, paper no. 128 (Houston, TX: NACE, 1990). 1990.

78. Braker, G., A. Fesefeldt, and K.-P. Witzel, *Development of PCR Primer Systems for Amplification of Nitrite Reductase Genes (nirK and nirS) To Detect Denitrifying Bacteria in Environmental Samples.* Appl. Environ. Microbiol., 1998. **64**(10): p. 3769-3775.

79. Nemati, M., G.E. Jenneman, and G. Voordouw, *Impact of nitrate-mediated microbial control of souring in oil reservoirs on the extent of corrosion.* Biotechnol. Prog., 2001. **17**(5): p. 852-9.

80. Zintel, T.P., G.J. Licina, and T.R. Jack, *Techniques for MIC Monitoring*, in *A Practical Manual on Microbiologically Influenced Corrosion*, J.G.S. II, Editor. 2001, NACE International: Houston, TX. p. 10.1-10.19.

81. NACE, *Field Monitoring of Bacterial Growth in Oilfield and Gas Systems.* NACE Standard TM0194-2004.

82. Little, B., P. Wager, and F. Mansfeld, *Microbiologically Influenced Corrosion of Metals and Alloys.* Int. Mat. Rev., 1991. **36**(6): p. 253-272.

83. Hernández-Gayosso, M.J., et al., *Microbial consortium influence upon steel corrosion rate, using the electrochemical impedance spectroscopy technique.* Materials and Corrosion, 2004. **55**(9): p. 676-683.

84. API, *Recommended Practice for Biological Analysis of Subsurface Injection Waters, American Petroleum Institute, Washington, D.C.,*. 1982.

85. Williams, W.A., J.H. Lobos, and W.E. Cheetham, *A phylogenetic analysis of aerobic polychlorinated biphenyl-degrading bacteria.* Int. J. Syst. Bacteriol., 1997. **47**(1): p. 207-10.

86. Maidak, B.L., et al., *The RDP-II (Ribosomal Database Project).* Nucleic Acids Res, 2001. **29**(1): p. 173-4.

87. Muyzer, G., E.C. de Waal, and A.G. Uitterlinden, *Profiling of complex microbial populations by denaturing gradient gel electrophoresis analysis of polymerase chain reaction-amplified genes coding for 16S rRNA.* Appl Environ Microbiol, 1993. **59**(3): p. 695-700.

88. Zhu, X.Y., T. Zhong, Y. Pandya, R. D. Joerger, *16S rRNA-based analysis of microbiota from the cecum of broiler chickens.* Appl. Environ. Microbiol., 2002. **68**(1): p. 124-37.

89. Osburne, M.S., T. H. Griossman, P. R. August, I. A. MacNeil, *Tapping into microbial diversity for natural products drug discovery.* ASM News, 2000. **66**: p. 411-417.

90. Torsvik, V., J. Goksoyr, and F.L. Daae, *High diversity in DNA of soil bacteria.* Appl Environ Microbiol, 1990. **56**(3): p. 782-7.

91. Harmsen, H.J., et al., *Population dynamics of propionate-oxidizing bacteria under methanogenic and sulfidogenic conditions in anaerobic granular sludge.* Appl. Environ. Microbiol., 1996. **62**(6): p. 2163-8.

92. Zhu, X.Y. and R.D. Joerger, *Composition of microbiota in content and mucus from cecae of broiler chickens as measured by fluorescent in situ hybridization with group-specific, 16S rRNA-targeted oligonucleotide probes.* Poult Sci, 2003. **82**(8): p. 1242-9.

93. Voordouw, G., *Reverse Sample Genome Probing of Microbial Community Dynamics.* ASM News, 1998. **64**: p. 627-633.

94. Voordouw, G., et al., *Application of Reverse Sample Genoma Probing to the Identification of Sulfate-Reducing Bacteria*, in *Microbiologically Influenced Corrosion Testing, ASTM STP 1232*, J.R. Kearns and B.J. Little, Editors. 1994, Philadelphia, PA: ASTM. p. 188-199.

95. Telang, A.J., S. Ebert, J. M. Foght, D. W. S. Westlake, G. E. Jenneman, D. Gevertz, G. Voordouw, *Effect of nitrate injection on the microbial community in an oil field as monitored by reverse sample genome probing.* Appl. Environ. Microbiol., 1997. **63**(5): p. 1785-1793.

96. Skovhus, T.L., et al., *Real-Time Quantitative PCR for Assessment of Abundance of Pseudoalteromonas Species in Marine Samples.* Appl. Environ. Microbiol., 2004. **70**(4): p. 2373-2382.

97. Stults, J.R., O. Snoeyenbos-West, B. Methe, D. R. Lovley, D. P. Chandler, *Application of the 5' fluorogenic exonuclease assay (TaqMan) for quantitative ribosomal DNA and rRNA analysis in sediments.* Appl. Environ. Microbiol., 2001. **67**(6): p. 2781-2789.

98. Suzuki, M.T., L.T. Taylor, and E.F. DeLong, *Quantitative Analysis of Small-Subunit rRNA Genes in Mixed Microbial Populations via 5'-Nuclease Assays.* Appl. Environ. Microbiol., 2000. **66**(11): p. 4605-4614.

99. Brinkman, N.E., et al., *Evaluation of a Rapid, Quantitative Real-Time PCR Method for Enumeration of Pathogenic Candida Cells in Water.* Appl. Environ. Microbiol., 2003. **69**(3): p. 1775-1782.

100. Guy, R.A., et al., *Real-Time PCR for Quantification of Giardia and Cryptosporidium in Environmental Water Samples and Sewage.* Appl. Environ. Microbiol., 2003. **69**(9): p. 5178-5185.

101. Ibekwe, A.M., et al., *Multiplex Fluorogenic Real-Time PCR for Detection and Quantification of Escherichia coli O157:H7 in Dairy Wastewater Wetlands.* Appl. Environ. Microbiol., 2002. **68**(10): p. 4853-4862.

102. Blackburn, F.E., *Non-Bioassay Techniques for Monitoring SRB.* CORROSION/2004 (Houston, TX: NACE, 2004).

103. Dorsey, M.H., et al., *Monitoring for Corrosion and Microbiological Activity in a Cooling Water System.* Plant Power Chemistry, 2002. **4**(12): p. 721-731.

104. Royer, R.A. and R.F. Unz, *Use of Electrical Resistance Probes for Studying Microbiologically Influenced Corrosion.* Corrosion, 2002. **58**(10): p. 863-870.

105. Pope, D.H., *State-of-the-Art Report on Monitoring, Prevention and Mitigation of Microbiolwically lnfluenced Corrosion in the Natural Gas Industrv.* Topical Report, GRI-9210382. Gas Research Institute, Chicago, IL, 1992.

106. Lockwood, S.F., et al., *Microbiologically lnfluenced Corrosion in the Natural Gas Industry.* Topical Report (Unpublished) to Gas Research Institute, February 1993., 1993.

107. Lutey, R.W., *Treatment for the Mitigation of MIC*, in *A Practical Manual on Microbiologically Influenced Corrosion*, J.G. Stoecker, Editor. 1993, Houston, TX: NACE. p. 9.1-9.9.30.

108. Nichols, W.W., et al., *The penetration of antibiotics into aggregates of mucoid and non-mucoid Pseudomonas aeruginose.* J. Gen. Microbiol., 1989. **35**(35): p. 1219-1303.

109. Kajdasz, R.E., R.V. Einstman, and L. Young-Bandala, *Biocidal Efficacy with Respect to Sessile and Planktonic.* IWV, 1984: p. 85-93.

110. McCoy, W.F., *Strategies for the treatment of biological biofouling.*, in *Biological fouling of industrial water systems - A problem solving approach*, M.W. Mittelman and G.G. Geysey, Editors. 1987, Water Micro. Associates: San Diego, CA. p. 247-268.

111. Pope, D.H. and R. Skultety, *Microbiologically lnfluenced Corrosion in Natural Gas Storage Fields: Diagnosis, Monitoring and Control.* NACE International Conference on Microbiologically lnfluenced Corrosion, Paper No. 57. New Orleans, LA., 1995.

112. Webster, B.J. and R.C. Newman, *ASTM STP 1232: Producing Rapid Sulfate-Reducing Bacteria-Influenced Corrosion in the Laboratory*, in *Microbiologically Influenced Corrosion Testing*, J. Kearns and B.J. Little, Editors. 1994, ASTM: West Conshohocken, PA. p. 28-41.

113. Little, B. and R. Ray, *A Perspective on Corrosion Inhibition by Biofilms.* Corrosion, 2002. **58**(5): p. 424-428.

114. Jayaraman, A., et al., *Axenic aerobic biofilms inhibit corrosion of copper and aluminum.* Appl Microbiol Biotechnol., 1999. **52**(6): p. 787-790.

115. Jayaraman, A., et al., *Inhibiting sulfate-reducing bacteria in biofilms on steel with antimicrobial peptides generated in situ.* Appl Microbiol Biotechnol., 1999. **52**(2): p. 267-275.

116. Zuo, R., *Biofilms: strategies for metal corrosion inhibition employing microorganisms.* Appl Microbiol Biotechnol., 2007. **76**(6): p. 1245.

117. Zuo, R. and T.K. Wood, *Inhibiting mild steel corrosion from sulfate-reducing and iron-oxidizing bacteria using gramicidin-S-producing biofilms.* Appl Microbiol Biotechnol., 2004. **65**(6): p. 747-753.

118. Zuo, R., et al., *Inhibiting mild steel corrosion from sulfate-reducing bacteria using antimicrobial-producing biofilms in Three-Mile-Island process water.* Appl Microbiol Biotechnol., 2004. **64**(2): p. 275-283.

119. Chan, K.Y., L.C. Xu, and H.H. Fang, *Anaerobic electrochemical corrosion of mild steel in the presence of extracellular polymeric substances produced by a culture enriched in sulfate-reducing bacteria.* Environ Sci Technol., 2002. **36**(8): p. 1720-1727.

120. Hernandez, G., et al., *Corrosion Inhibition of Steel by Bacteria*. Corrosion, 1994. **50**(08): p. 603-608.

121. Jayaraman, A., et al., *Axenic Aerobic Biofilms Inhibit Corrosion of SAE 1018 Steel through Oxygen Depletion.* Applied Microbiology and Biotechnology, 1997. **48**: p. 11-17.

122. McCafferty, E. and J.V. McArdle. *Corrosion Inhibition by Biological Siderophore*. in *182nd Society Meeting (Toronto, Canada: The Electrochemical Society)*. 1992.

123. Eashwar, M. and S. Maruthamuthu, *Mechanism of biologically produced ennoblement: Ecological perspectives and a hypothetical model.* Biofouling, 1995. **8**(3): p. 203-213.

124. Little, B., P. Wagner, and F. Mansfeld, *Microbiologically Influenced Corrosion of Metals and Alloys.* Int. Mat. Rev., 1991. **36**(6): p. 253-272.

125. Geesey, G.G., in *Biofouling and biocorrosion in industrial water systems*, H.-C. Flemming and G.G. Geesey, Editors. 1991, Springer-Verlag: Berlin.

126. Heitz, E., in *Microbially influenced corrosion of materials*, E. Heitz, H.-C. Flemming, and W. Sand, Editors. 1996, Springer-Verlag: Berlin, New York.

127. AGA, *American Gas Association. Transmission Measurement Committee. AGA Report No. 4A, Natural Gas Contract Measurement and Quality Clauses – 2008 DRAFT. Washington, DC: American Gas Association, 2008*. 2008.

128. Alexander, B. and F.G. Priest, *Bacillus glucanolyticus, a new species that degrades a variety of beta-glucans.* Int. J. Syst. Bacteriol., 1989. **39**: p. 112-115.

129. Pridal, A., *Microorganisms in Dead Bumble Bee Larvae (Bombus spp.) from Laboratory-Reared Colonies.* ACTA Universitatis Agriculturae et Silviculturae Mendelianae Brunensis, 2001(5): p. 41-48.

130. http://en.wikipedia.org/wiki/Bacillus_licheniformis.

131. Scheldeman, P., et al., *Incidence and Diversity of Potentially Highly Heat-Resistant Spores Isolated at Dairy Farms 10.1128/AEM.71.3.1480-1494.2005.* Appl. Environ. Microbiol., 2005. **71**(3): p. 1480-1494.

132. Little, B.J., J.S. Lee, and R.I. Ray, *Diagnosing Microbiologically Influenced Corrosion: A State-of-the-Art Review.* Corrosion, 2006(62): p. 1006.

133. Pots, B.F.M. and S.D. Kapusta, *Prediction of Corrosion Rates of the Main Corrosion Mechanisms in Upstream Applications.* Nace International Corrosion 2005. Paper No. 05550., 2005: p. 1-21.

134. Crolet, J.-L., *Observation of Non-SRB Sulfidogenic Bacteria from Oilfield Production Facilities.* CORROSION/95, paper no. 188 (Houston TX, NACE, 1995). 1995.

135. Crolet, J.-L., *From the General Mechanism to Specific Mechanisms of Localized Corrosion*, in *Localized Corrosion*, F. Dabosi, G. Beranger, and B. Baroux, Editors. 1994, Les Editions de Physique: Les Ulis, France.

136. Crolet, J.-L., S. Daumas, and M. Magot, *pH Regulation by Sulfate-Reducing Bacteria.* CORROSION/93, paper no. 303 (Houston TX: NACE), 1993.

137. Lee, W., et al., *Role of Sulfate-Reducing Bacteria in Corrosion of Mild Steel: A Review.* Biofouling, 1995. **8**: p. 165-194.

138. Newman, R.C., B.J. Webster, and R.G. Kelly, *The electro- chemistry of SRB corrosion and related inorganic phenomena.* ISIJ Int, 1991. **31**: p. 201-209.

139. Yang, B., *Localized Corrosion Monitoring in Cooling Water Systems.* CORROSION/95, paper no. 541 (Houston, TX: NACE, 1995). 1995.

140. Walt, D.R., et al., *The effect of gravity on initial microbial adhesion.* J. Colloidal Interface Sci, 1985. **107**(2): p. 334-336.

141. Marmur, A. and E. Ruckenstein, *Gravity and cell adhesion.* Journal of Colloid and Interface Science, 1986. **114**(1): p. 261-266.

142. Picioreanu, C. and M.C.M.v. Loosdrecht, *A Mathematical Model for Initiation of Microbiologically Influenced Corrosion by Differential Aeration.* J. Electrochemical Society, 2002. **149**(6): p. B211-B223.

143. Sooknah, R., S. Papavinasam, and R.W. Revie, *Validation of a Predictive Model for Microbiologically Influenced Corrosion, NACE/2008, Paper 08503.*

144. King, F., *Microbiologically Influenced Corrosion of Nuclear Waste Containers.* Corrosion, 2009. **65**(4): p. 233-251.

145. Zhao, K., J. Wen, and T. Gu, *Mechanistic Modeling of Anaerobic THPS Degradation in Seawater Under Various Conditions, NACE/08, Paper 08512.*

146. Gu, T., K. Zhao, and S. Nesic, *A New Mechanistic Model for MIC Based on a Biocatalytic Cathodic Sulfate Reduction Theory, NACE/09, Paper 09390.* 2009.

147. Song, F.M. and N. Sridhar, *Modeling Pipeline Crevice Corrosion under a Disbonded Coating with or without Cathodic Protection under Transient and Steady-State Conditions.* Corrosion Science, 2008. **50**(1): p. 70-83.

148. Song, F.M. and N. Sridhar, *Modeling Pipeline Corrosion under a Disbonded Coating under the Influence of Underneath Flow.* Corrosion, 2008. **64**(1): p. 40-50.

149. Song, F.M. and N. Sridhar, *A Two-Dimensional Model for Steel Corrosion under a Disbonded Coating due to Oxygen with or without Cathodic Protection-Part 1: Full Numerical Solution.* Corrosion, 2006. **62**(8): p. 676-686.

150. Song, F.M., D.A. Jones, and D.W. Kirk, *Corrosion and Current Flow within a Pipeline Disc Crevice.* Corrosion, 2005. **62**(2): p. 145-154.

151. Song, M., et al., *CO2 Corrosion of Bare Steel under an Aqueous Boundary Layer with Oxygen and Cathodic Protection.* Corrosion, 2004. **60**(9): p. 845-851.

152. Song, F.M., et al., *CO2 Corrosion of Bare Steel under an Aqueous Boundary Layer with Oxygen.* Journal of The Electrochemical Society, 2002. **149**(11): p. B479-B486.

153. Song, F.M., et al., *CO2 Corrosion of Bare Steel under an Aqueous Boundary Layer.* Corrosion, 2004. **60**(8): p. 736-748.

154. Song, F.M., *Exploring to Predict Pipeline High-pH SCC Crack Growth Rate, Sept. 29-Oct. 3, 2008, ASME IPC 2008, Paper 64671 (A Best Conference Paper).* 2008.

155. Song, F.M., *Overall Mechanisms of High pH and Near-Neutral pH SCC, Models for Forecasting SCC Susceptible Locations, and Simple Algorithms for Predicting High pH SCC Crack Growth Rates. March 16-20, 2008 (Houston, TX: NACE, 2008) Paper: 08129.* 2008.